AD_____

GRANT NUMBER DAMD17-96-1-6149

TITLE: Control of Breast Tumor Cell Growth by Dietary Indoles

PRINCIPAL INVESTIGATOR: Leonard Bjeldanes

CONTRACTING ORGANIZATION: University of California
Berkeley, CA 94720-5940

REPORT DATE: September 1998

TYPE OF REPORT: Annual

PREPARED FOR: Commander
U.S. Army Medical Research and Materiel Command
Fort Detrick, Frederick, Maryland 21702-5012

REPORT DOCUMENTATION PAGE

Form Approved
OMB No. 0704-0188

1. AGENCY USE ONLY *(Leave blank)*	2. REPORT DATE	3. REPORT TYPE AND DATES COVERED
	September 1998	Annual (1 Sep 97 - 31 Aug 98)

4. TITLE AND SUBTITLE
Control of Breast Tumor Cell Growth by Dietary Indoles

5. FUNDING NUMBERS
DAMD17-96-1-6149

6. AUTHOR(S)
Leonard Bjeldanes

7. PERFORMING ORGANIZATION NAME(S) AND ADDRESS(ES)
University of California
Berkeley, California 94720-5940

8. PERFORMING ORGANIZATION REPORT NUMBER

9. SPONSORING/MONITORING AGENCY NAME(S) AND ADDRESS(ES)
U.S. Army Medical Research and Materiel Command
Fort Detrick, Maryland 21702-5012

10. SPONSORING/MONITORING AGENCY REPORT NUMBER

19981229 116

11. SUPPLEMENTARY NOTES

12a. DISTRIBUTION / AVAILABILITY STATEMENT
Distribution authorized to U.S. Government agencies only (proprietary information, Sep 98). Other requests for this document shall be referred to U.S. Army Medical Research and Materiel Command, 504 Scott Street, Fort Detrick, Maryland 21702-5012.

12b. DISTRIBUTION CODE

13. ABSTRACT *(Maximum 200 words)*

Indole-3-carbinol (I3C), a naturally occurring component of Brassica vegetables, has been shown to reduce the incidence of spontaneous and carcinogen-induced mammary tumors. Our studies of the molecular mechanisms and signal transduction pathways by which I3C mediates its antiproliferative effects have established that, **a)** DIM, a major in vivo conversion product of I3C can exhibit both agonist and antagonist activities against proliferation of MCF-7 cells and against transcriptional activation of endogenous and exogenous estrogen-responsive genes. Under conditions where cells are exposed to both DIM and estrogen, the primary effect of DIM is antagonistic of estrogen function and this effect appears to be independent of the Ah receptor. **b)** A second major component of RXM, the linear trimer, 2-(indol-3-ylmethyl)-3,3´-diindolylmethane (LTr-1), is an antagonist of estrogen receptor function with little agonist activity. LTr-1 is a strong inhibitor of proliferation of both estrogen dependent and independent cultured breast tumor cells. **c)** I3C and tamoxifen work through different signal tranduction pathways to suppress the growth of human breast cancer cells. Most significantly, a combination of tamoxifen and I3C displayed a more effective growth suppression response, more stringent inhibition of CDK2 specific activity, and more endogenous Rb phosphorylation compared to the effects of either compound alone.

14. SUBJECT TERMS	15. NUMBER OF PAGES
antiestrogen, estrogen receptor, gene regulation, dietary indoles, Ah receptor, cell cycle arrest	43
	16. PRICE CODE

17. SECURITY CLASSIFICATION OF REPORT	18. SECURITY CLASSIFICATION OF THIS PAGE	19. SECURITY CLASSIFICATION OF ABSTRACT	20. LIMITATION OF ABSTRACT
Unclassified	Unclassified	Unclassified	Limited

FOREWORD

Opinions, interpretations, conclusions and recommendations are those of the author and are not necessarily endorsed by the U.S. Army.

____ Where copyrighted material is quoted, permission has been obtained to use such material.

____ Where material from documents designated for limited distribution is quoted, permission has been obtained to use the material.

____ Citations of commercial organizations and trade names in this report do not constitute an official Department of Army endorsement or approval of the products or services of these organizations.

(LB)✓ In conducting research using animals, the investigator(s) adhered to the "Guide for the Care and Use of Laboratory Animals," prepared by the Committee on Care and use of Laboratory Animals of the Institute of Laboratory Resources, national Research Council (NIH Publication No. 86-23, Revised 1985).

(LB)✓ For the protection of human subjects, the investigator(s) adhered to policies of applicable Federal Law 45 CFR 46.

____ In conducting research utilizing recombinant DNA technology, the investigator(s) adhered to current guidelines promulgated by the National Institutes of Health.

____ In the conduct of research utilizing recombinant DNA, the investigator(s) adhered to the NIH Guidelines for Research Involving Recombinant DNA Molecules.

____ In the conduct of research involving hazardous organisms, the investigator(s) adhered to the CDC-NIH Guide for Biosafety in Microbiological and Biomedical Laboratories.

Leonard Bjeldanes 9/25/98

PI - Signature Date

Table of Contents

Introduction:

Indole-3-carbinol (I3C) is a naturally occurring component of dietary vegetables and a promising cancer preventive agent, most notably against breast cancer. I3C markedly reduces the incidence of spontaneous and carcinogen-induced mammary tumors in rodents and exhibits potent growth inhibitory activity in human breast cancer cells. Although I3C has reached the stage of phase I clinical trials, little is known about the mechanism of its growth inhibitory effects in cancer cells. The purpose of this work is to establish the mechanism of action and to exploit the cancer preventive properties of I3C and related compounds.

I3C is active in several key anticancer-related bioassays. Rodents exposed to high doses of I3C via oral intubation or diet exhibited increases in the activities of a variety of cytochrome P-450-dependent activities including hepatic ethoxyresorufin O-deethylase (EROD) and related activities (1,2). I3C reduced BP-induced neoplasia of the forestomach (3) and total covalent binding of BP and N-nitrosodimethylamine to hepatic DNA in mice (4,5,6). In trout, I3C reduced AFB1-induced hepatocarcinogenesis when administered prior to and during carcinogen treatment (7). In a recent screen of 90 potential chemopreventive agents in a series of 6 short term bioassays relevant to carcinogen-induced DNA damage, tumor initiation and promotion, and oxidative stress, I3C was found to be one of only 8 compounds that tested positive in all assays. The authors of this study opined that I3C was highly promising for development as a cancer chemopreventive agent (8).

Some of the most well established biological effects of I3C appear to be related to its antiestrogenic effects. In a long term feeding experiment, in which female mice consumed synthetic diets containing I3C at 0, 500 or 2000 p.p.m., spontaneous mammary tumor incidence and multiplicity were significantly lower (ca. 50% reduction) at both doses of I3C than for untreated control animals, and tumor latency was prolonged in the high dose group (9). Oral administration of I3C to humans at doses of around 500 mg daily for one week produced an increase in estradiol 2-hydroxylation of approximately 50% in both men and women (10). I3C also increased the levels of estradiol hydroxylation activity in female rats (11).

The effects of I3C on DMBA-induced mammary tumors in rodents were reported in two studies. Wattenberg reported that I3C administered in the diet or by oral intubation prior to treatment with carcinogen reduced tumor incidence by 70-80% (3). In a recent study by Lubet, I3C administered prior to and during DMBA treatment reduced mammary tumor incidence by as much as 95% in rats (12). In a post-initiation protocol, I3C administration following treatment with NMU reduced tumor incidence by 65% (12). Consistent with these results, supplementation of a purified diet with cabbage or broccoli, both of which vegetables are good sources of I3C, also resulted in decreased mammary tumor formation in DMBA-treated rats (13).

The antiestrogenic growth suppressive effects of I3C are also established for breast tumor cells in culture. Estradiol-induced proliferation of high density human MCF-7 cells was totally blocked by 50 μM I3C in the growth medium. I3C did not affect the proliferation of the estrogen-independent breast tumor line MDA-MB-231 in this experiment (14).

Because of these well documented cancer protective effects of I3C, along with its effects on estrogen metabolism, its low toxicity, and its wide availability, I3C is currently undergoing at least two different phase I clinical trials as a cancer chemotherapeutic and preventive agent (12).

Our working hypothesis is that I3C stimulates changes in the expression and activity of a network of early-response regulatory molecules that control a subsequent cascade of events leading to the arrest of human mammary tumor cell growth. We suggest further that one result of

activation of this cascade is the blockade of estrogen-induced signal transduction pathways central to cell growth and proliferation.

Body:

1. Results and Discussion.

Progress was made under each of the stated objectives and three new manuscripts have been submitted. Our manuscript describing the estrogen-independent cell cycle effects of I3C has been published (15).

I. Identify I3C products that are responsible for I3C's growth inhibitory effects in breast tumor cells. Our initial studies of I3C products began with DIM because it is a major in vivo and in vitro conversion product of I3C and it is readily available by straight forward synthetic procedures. Further studies of the indole reaction mixture (RXM) have resulted in the identification of the indole linear trimer (LTr-1) as a potent cytostatic agent in the MCF-7 human breast cancer cell line.

A. 3,3'-Diindolylmethane inhibits the estrogen-enhanced proliferation of human breast cancer cells but promotes their growth in the absence of estrogen. The effects of DIM on MCF-7 cell proliferation are summarized in Figure 1. DIM by itself increases cell growth in a dose-dependent manner after either 4-day or 7-day treatment. In the presence of estrogen, however, DIM (10 uM) inhibits estrogen-stimulated cell growth up to 50% after 7 days. In contrast, DIM had little effect on proliferation of an estrogen receptor deficient breast tumor-derived cell line, MDA-MB-231, producing only a 15% decrease in cell number after 7 days at a concentration of 10 uM (data not shown). This result indicates that the growth inhibitory effects of DIM in MCF-7 cells are, at least in part, estrogen receptor dependent.

B. 2-(Indol-3-ylmethyl)-3,3′-diindolylmethane is a major cytostatic product of dietary indole-3-carbinol.

a. Fractionation of RXM. Silica gel vacuum liquid chromatography was used for the initial crude fractionation of RXM. Five fractions were collected, 100% hexane (A), hexane/THF 2:1 (B), hexane/THF 1:1 (C), hexane/THF 1:1 (D) and 100% THF (E), with gradually increasing mobile phase polarity. At a concentration 50 μM (I3C equivalent) based on weight of residual material after evaporation of solvent, all five fractions inhibited MCF-7 cell proliferation in the presence of 1 nM of estrogen. Fraction B, the chromatogram of which contained a predominant peak and many minor peaks (Figure 1), was further purified on a reverse-phase semi-preparative HPLC column using the conditions described in the experimental section. Of the nine major fractions collected, fraction Bc exhibited the strongest toxic and antiproliferative activities against MCF-7 cells. In several experiments, crude RXM inhibited cell proliferation by about 50% at the highest non-lethal concentrations (Figure 2).

HPLC analysis of fraction Bc (Figure 3) indicated that it contained a single compound with a retention time of LTr-1 identified previously as a major component of RXM (2,16). Mass spectrometric analysis confirmed this structural assignment.

b. Cell proliferation studies of LTr-1. Results of tumor cell growth experiments showed that proliferation of both the estrogen dependent (MCF-7) and the estrogen independent (MDA) breast tumor cell lines were inhibited by LTr-1 by up to 60% in a concentration dependent manner (Figure 4). Furthermore, LTr-1 exhibited no stimulation of cell proliferation in the

absence of estrogen. The decreased cell counts were apparently not due to a general toxicity of the trimer since we saw no evidence of cell killing over the 7 day treatment period.

C. Indole-3-carbinol and tamoxifen cooperate to arrest the cell cycle of MCF-7 human breast cancer cells.

a. I3C and tamoxifen cooperate to arrest the growth of MCF-7 cells. To determine the potential combinatorial effects of I3C and tamoxifen on the growth of an estrogen-dependent breast cancer cell line, MCF-7 cells were grown in medium supplemented with 10% fetal bovine serum, which contains enough estrogen to support the proliferation of these cells. The cells were treated with 100 μM I3C, 1 μM tamoxifen, or a combination of I3C and tamoxifen, over a 96-hour time course (Fig. 5).

These concentrations of I3C and tamoxifen were previously shown to decrease cell growth without affecting viability (15,17). The cells were then pulse-labeled with [^{3}H]thymidine for three hours at each time point to provide a measure of their proliferative state. Analysis of [^{3}H]thymidine incorporation revealed that tamoxifen caused a steady decrease in DNA synthesis over the time course with a 60% inhibition after 96 hours of treatment. I3C treatment also resulted in a time-dependent decrease in DNA synthesis with a 90% inhibition after 96 hours. The combination of I3C and tamoxifen yielded statistically similar results as I3C alone for the 24 and 48 hour time points, however, by the 72 and 96 hour time points, the combination of I3C and tamoxifen resulted in a more effective growth suppression than either agent alone, resulting in a 95% inhibition after 96 hours of treatment.

b. Effects of I3C and tamoxifen on adherent cell growth, anchorage independent cell growth, and morphology. To characterize the inhibitory effects of I3C and tamoxifen on adherent cell growth, MCF-7 cells were plated at low confluency (10,000 single cells per 100 mm plate) and grown for 8 days in medium containing the vehicle control or various doses of each agent alone or in combination. To visualize the cell colonies, the cells were stained and fixed in crystal violet/formalin. Representative plates of vehicle control, high doses of I3C (100 μM) or tamoxifen (1 μM) and the combination of I3C and tamoxifen are shown in figure 6A. The average integrated density of replicate areas on each plate was determined by NIH Image and normalized by dividing that value by the area which was measured on each plate. This measurement takes into account both the number and size of the colonies, and is representative of the number of cells on each plate. Treatment with the high doses of I3C or tamoxifen alone inhibited cell colony formation by 80% and 65%, respectively, whereas, a combination of both agents inhibited adherent cell growth by greater than 95%. An expanded analysis of the dose dependent suppression of adherent cell growth by I3C and tamoxifen is shown in figure 6C.

The effects of combinations of I3C and tamoxifen on the anchorage independent growth of MCF-7 cells in soft agar was examined. Cells were cultured for 4.5 weeks in 0.3% agar and complete media containing the vehicle control, I3C, tamoxifen or a combination of both agents, and cell colonies larger than 50 μm in diameter were counted. As shown in figure 6D, increasing doses of I3C or tamoxifen caused a decrease in cell colony formation and, consistent with the adherent cell growth properties, a combination of both agents caused a more pronounced decrease in cell colony formation. For both growth conditions, the combined inhibitory effect of suboptimal concentrations of I3C (50 μM) and tamoxifen (0.5 μM) approximated that observed with the highest doses of either I3C or tamoxifen alone.

The morphology of the cells within the adherent colonies (Fig. 6A) was visualized at 200 fold magnification (Fig. 6B). It is evident that each cell colony on the vehicle control-treated

plates contain more cells than the corresponding colonies of tamoxifen- and I3C-treated plates. In addition, both growth suppressers altered the morphology of MCF-7 cells. I3C-treated cells appeared larger and more flattened than the vehicle control-treated cells with protrusions of the plasma membrane. Tamoxifen-treated cells displayed a different morphology than the I3C-treated, although the cell size appeared to be between that observed for the vehicle control-treated cells and the I3C-treated cells. Treatment with a combination of tamoxifen and I3C induce a morphology change similar to the cells treated with I3C alone. Consistent with the reversible growth arrest observed with I3C treatment (18), the release from I3C caused the cell morphology to return to that of vehicle control-treated cells (data not shown).

c. Cell cycle effects of I3C and tamoxifen. To assess the effect of combinations of I3C and tamoxifen on the cell cycle, MCF-7 cells were treated with the indicated concentrations of each compound for 96 hours and then hypotonically lysed in the presence of propidium iodide to stain the nuclear DNA. Flow cytometry profiles revealed that treatment with increasing doses of I3C or tamoxifen lead to a dose-dependent shift in percentage of cells with a G1-like DNA content. As shown in figure 7A, I3C or tamoxifen altered the DNA content of the MCF-7 cell population from an asynchronous population of growing cells in all phases of the cell cycle (61.4% in G1, 29.0% in S phase, and 9.7% in G2/M phase) to one in which most of the treated breast cancer cells were in the G1 phase of the cell cycle (Fig. 7A, upper right panel for I3C and lower left panel for tamoxifen). Consistent with the cell growth studies, a combination of both agents caused a more striking shift to the G1-phase of the cell cycle (Fig. 7A, lower right panel). Consistent with the growth assays shown in figure 6, incubation with suboptimal concentrations of both I3C and tamoxifen (Fig. 7A, middle panel) induced the G1 shift to approximately the same extent as observed with the highest concentrations of either compound alone. As shown graphically in figure 7B, the I3C- and tamoxifen-mediated shift in number of G1 phase cells (upper panel) appears to result from a decrease in S-phase cells (middle panel) while the G2/M phase values do not significantly change (lower panel).

The expression levels of specific cell cycle proteins that are responsible for progression through G1 and/or transition into S phase were examined in cells treated for 96 hours with combinations of 100 μM I3C and/or 1 μM tamoxifen. Western blot analysis revealed that I3C selectively decreased the level of CDK6 protein and increased the level of the p21 CDK inhibitor (Fig. 8). In contrast, tamoxifen had no effect on each of these cell cycle proteins under our cell culture conditions. The expression of the other cell cycle proteins tested, such as CDK2, CDK4, cyclin D1, and cyclin E were not affected by either I3C or tamoxifen.

d. I3C and tamoxifen cooperate to decrease the *in vitro* activity of CDK and the phosphorylation of endogenous Rb. The control of G1 CDK enzymatic activity is critical for regulating cell cycle progression (18). The activity of specific CDKs is regulated, in part, by the composition of the holoenzyme, which includes the appropriate cyclin and/or CDK inhibitory proteins. Therefore, even though the levels of CDK2 and CDK4 remain unaltered after I3C and/or tamoxifen treatment, we examined the potential effects of I3C and tamoxifen on G1 CDK specific activities. Because one of the key endogenous substrates for the G1 CDKs is the Rb protein, we determined the ability of the individual G1 CDKs to phosphorylate Rb *in vitro*. MCF-7 cells were treated for 48 hours with I3C and/or tamoxifen and then CDK2, CDK4, or CDK6 were then immunoprecipitated from total cell extracts. For the kinase assays, half of each immunoprecipitated sample was incubated with the carboxy-terminal domain of Rb fused to GST, and [γ^{33}P]ATP. The electrophoretically fractionated reaction products were

quantitated on a PhosphorImager and then visualized by autoradiography. The other half of the immunoprecipitated samples were analyzed by western blot and densitometry to confirm the efficiency and specificity of each immunoprecipitation. The CDK specific activity was calculated by dividing the *in vitro* kinase activity by the corresponding protein expression. As shown in the CDK2 specific activity graph, increasing doses of I3C alone or tamoxifen alone resulted in dose-dependent decreases in CDK2 specific activity (Fig. 9). Treatment with combinations of these two growth inhibitors resulted in a more stringent decrease in CDK2 specific activity than either agent alone. In contrast, I3C inhibited CDK6 protein expression but the specific activity of the residual CDK6 protein remained unaltered. Tamoxifen had no effect on CDK6 protein expression or specific activity (Fig. 9). Thus, the decrease in CDK6 activity appears to result from the I3C-mediated decrease in CDK6 protein levels and not due to an effect on CDK6 enzymatic activity. CDK4 specific activity was not affected by either tamoxifen or I3C (data not shown).

It was important to determine whether the *in vitro* kinase assay results reflected the phosphophoryation status of endogenous Rb after treatment with the antiproliferative agents. Therefore, the levels of phosphorylated and hypophosphorylated Rb were examined in MCF7 cells treated for 48 hours with I3C, tamoxifen, or a combination of both agents. The extent of Rb phosphorylation was determined by probing western blots with a Rb-specific antibody and analyzing the characteristic mobility shift of the hyperphosphorylated Rb protein. As shown in figure 10, I3C treatment, and to a lesser extent tamoxifen treatment, caused a decrease in total Rb protein levels and an increase in the relative levels of hypophosphorylated Rb (pRb). Most significantly, a combination of I3C and tamoxifen virtually ablated the expression of the hyperphosphorylated form of Rb (ppRb), which likely explains the more potent growth arrest observed in the presence of these two growth suppressors.

II. Characterize effects of I3C products on estrogen receptor- and Ah receptor-mediated cellular responses.

A. 3,3'-Diindolylmethane is a promoter specific partial agonist of estrogen receptor function in human breast cancer cells. The relative binding affinity of DIM to the estrogen receptor (ER) was measured by a competitive binding assay using 1.0 nM 3H-estradiol as the labeled ligand (Fig. 11). The IC50, the concentration of competitor necessary to displace the labeled ligand by 50%, was 3.0 nM, 200 nM and 75 μM for estradiol, tamoxifen, and DIM, respectively. The binding affinity of DIM relative to estradiol is 0.025.

Binding of the ER to its cognate DNA motif (ERE) was studied by a gel mobility shift assay using nuclear extracts from MCF-7 cells treated with estrogen, DIM, Tam, ICI, and various combinations of these, for 2.0 hours following a 7 day depletion period in 5% DCC-FBS to remove endogenous estrogens. A 31-mer 5'-32P double stranded oligonucleotide containing the consensus ERE motif was used as the labeled probe. Figure 12 shows that there was a marked ligand induced increase of binding with ER from nuclear extracts of cells treated with estradiol or DIM. These results indicate that DIM is a potentially significant ligand for the ER and is capable of activating ER binding to the ERE.

The promoter and cell specific effects of DIM on ER-responsive gene transcription were investigated using an endogenously expressed native gene and transiently transfected reporter constructs.

DIM behaves as an estrogen receptor agonist, inducing the expression of endogenous pS2 mRNA in a dose-dependent manner, while in the presence of estrogen, it has a slightly inhibitory effect on pS2 mRNA expression (Fig. 13). Analogous results were obtained in an analysis of DIM effects on expression of pEREvitCAT and pS2CAT reporters (Fig. 14 and Fig. 15), indicating that DIM functions at the level of transcriptional activation of complex promoters. DIM activated these genes to at least 50% the level induced by estrogen alone and DIM inhibited the activity of ESTROGEN by about 25%.

The dose-response results with vitCAT expression shown in figure 16 indicate that while treatment of cells with estrogen alone produced the normal dose-dependent increase in CAT activity, cotreatment with ESTROGEN had no effect on the suboptimal response produced by DIM. This result indicates that DIM functions independently of estradiol in a manner that is not successfully countered by high concentrations of estrogen.

To examine whether limited ER concentration could be a factor in the effects elicited by DIM, cells were cotransfected with pCMV-hER, an expression vector for the human estrogen receptor. The results indicated (data not shown) that over expression of ER did not affect the relative agonist or antagonist activities of estrogen and DIM.

The agonist effects of DIM observed with the complex promoters was not found however, when cells were transfected with the simpler estrogen and DES-responsive ERE-CAT reporter pATC2 (Fig. 17). This reporter was constructed by from the promoter region of the Xenopus vitallogenin II gene, and includes the two imperfect ERE motifs from that same gene. This observation indicates that the agonist effect of DIM is mediated by cis-acting elements in addition to the ERE.

We observed that the agonist effects of estrogen and DIM are affected differently by standard antiestrogens. The effects of two standard estrogen antagonists, tamoxifen and ICI182780 (ICI), on CAT activity induced by either DIM or estrogen with the ERE-vit-CAT reporter, are shown in figure 18. The dose response of ICI shows that this substance, considered a pure estrogen antagonist, inhibited transcription of CAT induced by DIM as well as by estrogen. ICI was a more effective inhibitor of DIM-induced activity than of estrogen-induced activity as indicated by the 77%reduction in the former and the 26% reduction in the latter produced by ICI at a concentration of 1 nM. Co-treatment of cells with tamoxifen and estrogen or DIM, however, produced distinctly divergent effects of ERE-vitCAT expression. While tamoxifen alone had no effect on transcription, it had a marked synergistic effect with estrogen induction and a clear inhibitory effect on DIM-induced transcription. The combined effect of Tam and DIM was to partially reduce the level of synergistically induced activity. This result indicates further that estrogen and DIM function by distinct mechanisms in the activation of ER-dependent processes.

We determined that the effects of DIM are independent of the Ah receptor signal transduction pathway. To examine the possible involvement of the Ah receptor pathway in the transcription activation activities of DIM, we performed the ERE-vit-CAT transfection experiments in murine hepatoma cell line Hepa1c1c7 (wt) and the ARNT-deficient mutant (B13). Treatment of cells cotransfected with the CAT reporter and an estrogen receptor expersion plasmid with DIM and/or estrogen produced agonist and antagonist activities in the two murine cell lines that were similar to the results from the human MCF-7 line (Fig. 19). In this system, however, the agonist effect of DIM was equal to that of estradiol. These results are

not consistent with a role of the AhR/ARNT pathway in the activities of DIM and indicate that any necessary coactivators or corepressors involved are present in murine liver as well as in human breast derived cells.

B. 2-(Indol-3-ylmethyl)-3,3′-diindolylmethane (LTr-1) is a major antiestrogenic product of dietary indole-3-carbinol. To determine whether LTr-1 may contribute to the established antiestrogenic activities of I3C, we examined the effects of LTr-1 on estrogen receptor binding and gene activation. The relative binding affinity of LTr-1 for the ER , as measured by a competitive binding assay, indicated an IC50 of approximately 70 μM compared to 200 nM and 3.0 nM measured for tamoxifen and estradiol, respectively (Fig. 20).
The effect of LTr-1 on the binding activity of ER to its cognate DNA motif was studied by gel mobility shift assay. LTr-1 showed a strong concentration dependent inhibitory effect on the estrogen-induced binding of ER to ERE with nearly complete loss of the shifted band at 10 μM LTr-1 (Figure 21). In the absence of estrogen, however, LTr-1 exhibited weak agonist activity on ERE binding to DNA.

To determine whether LTr-1 can affect transcription of estrogen responsive genes, we examined its effects on expression of the endogenous pS2 gene, often used as a marker of estrogen responsive breast tumors, and on the pERE-vit-CAT reporter construct transiently transfected into MCF-7 cells. The pERE-vit-CAT construct contains the promoter and 5' flanking region of the Xenopus vitellogenin gene upstream of the CAT structural gene. The results of Northern blot analysis indicated that estrogen induced transcription of pS2 was inhibited in a concentration dependent manner (approximately 50% at 10 μM) by LTr-1 (Figure 22). In the absence of estrogen, LTr-1 did not induce significant transcription of pS2. A similar inhibitory effect of LTr-1 was seen on estrogen-induced expression of the pERE-vit-CAT reporter construct (Figure 23). In this case, however, LTr-1 exhibited weak activation of this reporter in the absence of estrogen. Thus, LTr-1 can suppress activation of estrogen responsive genes at concentrations similar to those required for inhibition of estrogen activation of ER binding to the ERE.

C. I3C is not an effective competitor of estrogen for binding to the estrogen receptor. Because both I3C and the antiestrogen tamoxifen inhibited the growth of estrogen responsive breast cancer cells, we wanted to determine whether I3C has any effect on estrogen receptor ligand binding. An *in vitro* competition binding assay for receptor-ligand interactions was utilized to examine the relative affinities of I3C and tamoxifen for the estrogen receptor. As a control and point of reference for the relative ligand affinity, unlabeled β-estradiol was shown to effectively compete with [^{3}H]β-estradiol binding to the estrogen receptor, with half-maximal competition occurring at approximately 10 nM (Fig. 24). As expected, tamoxifen has a relatively high affinity for the estrogen receptor with a half maximal [^{3}H]β-estradiol displacement of approximately 200 nM. In contrast, I3C caused no significant displacement of [^{3}H]β-estradiol binding to the estrogen receptor, even at 1 mM. For the assays used in this study, the highest concentration of tamoxifen was 1 μM, which is within the range of β-estradiol competition, and the highest concentration of I3C was 100 μM, which does not compete with β-estradiol for receptor binding.

III. Identify genes involved in the I3C-mediated inhibition of growth of breast tumor cells.

In our continued efforts to identify key genes involved in the cytostatic effects of I3C and its products on breast cancer cells, we are examining the effects of I3C and DIM on gene expression using subtractive cloning techniques. Previously, we reported the potentially very important observation of down regulation of CDK6 transcription by I3C. Efforts are in progress to determine the basis for the observed inhibition of expression of this gene and its significance to in the blockage of cell proliferation. In a follow-up to our initial gene screening efforts that employed differential display methods, we were unable to confirm the differential expression of our candidates genes, other than for CDK6. The number of false positive clones that we have obtained was reduced with the very careful application of the substractive cloning method. Of the over thirty clones we have isolated, we have so far confirmed the differential expression of six uncharacterized genes and paraoxonase, all of which are induced in the I3C-treated cells. Paraoxonase is a hydrolytic enzyme involved in the detoxification of certain pesticides and its deficiency is associated with abnormal lipid metabolism. Our efforts to identify and characterize differentially expressed sequences will be further intensified in the coming years of the grant.

2. Experimental methods and procedures.

A. Cell Culture. The human breast adenocarcinoma MCF-7 and MDA and the murine hepatoma Hepa 1c1c7 cells were grown as adherent monolayers in Dulbecco's modified Eagle's medium (DMEM), supplemented to 4.0 g/L glucose , 3.7 g/L sodium bicarbonate in a humidified incubator at 37° C and 5% CO_2 and passaged at approximately 80% confluency. Cultures used in subsequent experiments were at less than 25 passages.

B. Cell proliferation. Before the beginning of the treatments, cells were depleted of estrogen for at least 7 days (7-10 days) in medium composed of DMEM base without phenol-red (Sigma), with 4 g/L glucose, 3.7 g/L sodium bicarbonate, and 5% calf serum twice stripped in dextran-coated charcoal and microfiltered, supplemented with non-essential amino acids (Gibco), 2 mM glutamine and 10 ng/ml insulin. During the depletion period, medium was changed every other day. Treatment were administered by addition of 1µL of 1,000X solution in DMSO per mL of Medium. Once the treatment period started, medium was changed repeatedly (every day in the case of I3C) to counter rapid loss of readily metabolized compounds.

C. Cell Counting. Cells were harvested by trypsinization and resuspended in complete medium. Aliquots were diluted 50 folds in Isoton II (Coulter) and 500 µL duplicates counted in a Coulter particle counter and averaged.

D. Estrogen Receptor Binding Assay. Rat uterine cytosol was prepared as described previously. Briefly, 2.5 g of uterine tissue from 5 Sprague Dawley rats (12 weeks old) was excised and placed on ice. The fresh tissue was homogenized with 30 mL of ice cold TEDG buffer(10 mM Tris pH 7.4, 1.5 mM EDTA, 1 mM DTT, 10% glycerol) using a Polytron at medium speed for 1 min on ice. The homogenate was centrifuged at 2,800 rpm, 10 min , 4°C. The supernate was transferred to ultracentrifuge tubes and centrifuged at 39000 rpm, 90 min, 4°C. The supernate was aliquoted, quickly frozen in a dry-ice/ethanol bath and stored at -80°C. Protein concentration of the uterine cytosol was 3 mg/mL, as measured by the Bradford assay using bovine serum albumin as the standard.

For each competitive binding assay, 5 µl of 20 nM ^{3}H-estradiol (NEN product # NET 137) in 50 % ethanol 10 mM Tris, pH 7.5, 10 % glycerol, 1mg/mL BSA,

and 1mM DTT was placed in a 1.5 mL microcentrifuge tube. Competitive ligands were added as 1.0 µl of 100 X solution in DMSO. After mixing, 95 µl of uterine cytosol was added, the tube were vortexed and incubated at room 4 °C for 2-3 hours.

Proteins were precipitated by addition of 100 µL of 50% hydroxylapatite (HAP) slurry equilibrated in TE (50 mM Tris pH 7.4, 1 mM EDTA, pH7.4) and incubation on ice for 15 min with vortexing every 5 min to resuspend hydroxylapatite. The pellet was washed with 1.0 mL ice cold wash buffer (40 mM Tris, pH7.4, 100 mM KCl, and centrifuged for 5 min at 10,000 rpm, 4°C. The supernatant was carefully aspirated and the pellet washed two more time with 1.0 mL of wash buffer. The final pellet was resuspended l in 200 µl ethanol and transferred to a scintillation vial. T he tube was washed with another 200 µl ethanol and add to the same counting vial. A negative control contained no uterine cytosol. Non specific binding was determined using a 100 fold (0.1 µM) unlabelled estradiol. Relative binding affinities were calculated using the concentration of competitor needed to reduce ^{3}H-estradiol binding by 50% as compared to the concentration of unlabelled estradiol needed to achieve the same result.

E. Transient Transfections with reporters. Transfections were done by the lipofection method using Lipofectamine (Gibco BRL), a mixture of polycationic and neutral lipids that bind to plasmid DNA and form a suspension of microvesicles in serum-free culture medium. After addition to culture plates the vesicles make contact with the cell membrane and facilitate the incorporation of the DNA into the cells. Cells were grown in 10% FBS-DMEM to subconfluency and transferred to 6 mm Petri plates 24 hours before transfection. The plates were seeded with appropriate number of cells to get 50-60% confluent at the time of transfection. For each 6 mm plate, 8µl of Lipofectamine was diluted with 92 µL of OptiMem serum free medium (Gibco). Plasmid DNA 0.1-1.0 µg was diluted in 100 µL of serum free medium. Lipid and plasmid dilutions were combined mixed gently and incubated at room temperature for 30 -45 min. Meanwhile plates were washed with 4 mL serum free medium and 2 mL serum free medium was added to each plate. The 200 µL of the lipid/DNA suspension above was added to each plate and mixed gently. The plates were returned to the incubator for 5 - 6 hours and 2 mL of medium containing 10% calf serum was added. The next day plates were refed with fresh medium (5% DCC-FBS) and start 48 hours treatment.

F. Chloramphenicol Acetyl Transferase (CAT) assay. The CAT assay was done using the mixed-phase method, a modification of the single phase extraction assay described by Seed et al., in which the hydrophobic product of the reaction—the acylated chloramphenicol—migrates into the organic phase constituted by the scintillation fluid. At the end of the 48 h treatment period, the transfected cells were harvested by scrapping with a rubber policeman, transferred with the medium to a conical 15 mL, centrifuged at 2000 rpm for 3 min, resuspended in 1 mL cold PBS, transferred to Eppendorf tube, centrifuged at 3000 rpm for 2 min and washed in PBS a second time. Cell pellets wee resuspended in 200µL of Tris 0.1 M pH 8.0 and lysed by 3 cycles of freeze/thaw (alternating 5 min in dry-ice/alcohol and 5 min at 37°C). Cell lysates were incubated at 65°C for 15 min to inactivate acylases and centrifuged at 14000 rpm for 8 min. A 165 µL aliquot of the cytosol was transfer to a 7 mL scintillation vial and a 20 µL aliquot was reserved for determination of protein concentration by the

Bradford assay. The substrate mixture (85 µL) was added to the scintillation vial to get final concentrations of 100 mM Tris.HCl pH 8.0, 250 nmoles chloramphenicol, 1 µCi ^{3}H-acetyl CoA [200mCi/mmol, NEN # NET-290L, NEN # NET-290L] in a total volume 250 µL and mixed thoroughly. The organic scintillation fluid (4 mL) [EconoFluor 2 Packard # 6NE9699] was added slowly to avoid mixing with the aqueous phase and the vials were incubated at 37°C for 1-2 hours or until sufficient counts were obtained.

G. RNA Extraction and Northern Blot Analysis. Total RNA was extracted using Tri-reagent. In short, cells were lysed and homogenized by addition of Tri-reagent; then chloroform was used for phase separation. After centrifugation, the upper water-soluble supernatant was collected and RNAs were precipitated by isopropanol, washed by 75% ethanol, and dissolved in a proper solution. Total RNAs were electrophorosed on a 1.2% agarose gel containing 3% formaldehyde and using MOPS as the running buffer. The gel was then washed gently with 10X SSC and blotted with a nylon membrane filter (Biorad Zeta membrane) overnight to transfer the RNA onto the membrane. Then RNA was fixed by using a UV cross-linker.

H. Nuclear extracts. Three near confluent (80-90%), 100 mm Petri plates were used for each treatment. DIM, estradiol, tamoxifen or ICI were added as 1,000X solution in DMSO. After two hours the plates were placed on ice and washed twice with 5 mL of hypotonic buffer, 10 mM Hepes pH 7.5 and incubated with 2 mL of Hepes for 15 min. Cells were harvested in 1 mL of MDH buffer (3 mM $MgCl_2$, 1 mM DTT, 25 mM Hepes, pH 7.5) with a rubber scrapper, homogenized with a loose fitting teflon pestle and centrifuged at 1,000 g for 4 min at 4°C. The pellets were washed twice with 3 mL of MDHK buffer (3mM $MgCl_2$, 1 mM DTT, 0.1 M KCl, 25 mM Hepes, pH 7.5), resuspended in 1 mL of MDHK and centrifuged at 3,000 rpm for 4 min at 4°C in a microcentrifuge. The pellets were resuspended in 100 µL of HDK buffer (25 mM Hepes, pH 7.5, 1 mM DTT, 0.4 M KCl), incubated for 20 min on ice with mixing every 5 min and centrifuged at 14,000 rpm for 4 min at 4°C. Glycerol was added to the supernatants to a concentration of 10% and aliquots of the nuclear extracts were stored at -80°C.

I. Gel Mobility Shift Assay. The following two complementary 31-mer oligonucleotides: 5'-GATCCCAGGTCACAGTGACCTGAGCTAAAAT-3' and 5'-GATCATTTTAGCTCAGGTCACTGTGACCTGG-3' containing the palindromic ERE consensus motif (underlined) were annealed and 5'end-labelled with ^{32}P. Nuclear extract (7 µg of proteins), were mixed with 90 ng poly dIdC, 25 mM Hepes, 1 mM DTT, 10% glycerol, 1 mM EDTA, 160 mM KCL) in a total volume of 21 µL. After incubation for 15 min at room temperature, 4 µL (100,000 cpm) end-labeled ^{32}P-ERE probe was added and incubated for another 15 min at room temperature. After addition of 2.8 µL of 10X Ficoll loading buffer (0.25% bromophenol blue, 25% ficoll type 400), 22 µL aliquots were loaded unto a pre-run non-denaturing 4.0 % polyacrylamide gel in TAE (67 mM tris, 33 mM Na acetate, 10 mM EDTA, pH 8.0) at 120 V for 2 hours. The gel was then dried and autoradiographed.

J. Preparation of Acid Reaction Mixture (RXM). The procedure reported by Gross and Bjeldanes (19) was followed for the preparation of RXM. Briefly, I3C (100 mg, Aldrich Chemical Co. Milwaukee, WI) was suspended in 1M HCl (100 ml) at room temperature for 15 min. The acid suspension was neutralized with aqueous ammonia to pH 6.5 and the precipitate was filtered and air-dried to give RXM as a reddish powder.

K. Fractionation of RXM. RXM (200 mg) was dissolved in THF (1 ml) and purified by silica gel vacuum liquid chromatography. Mixtures of hexane/THF were used as mobile phase.

HPLC purification of bioactive components of the crude fractions was performed using a Shimadzu HPLC system equipped with a C-18 bond-phase semi-preparative column (Beckman Ultrasphere-ODS, 10 x 250 mm, 5 mm or 10 mm)(Beckman , San Ramon, CA) and UV/VIS detector . The peaks were monitored at 280 nm. Isocratic mixtures of acetonitrile/water 60:40 or 70:30 at a flow rate of 2 ml/min were used as mobile phases. Crude RXM fractions were extracted with hexane to remove lipophilic components and resuspended in THF before injection into HPLC.

The mass spectrum of LTr-1 was consistent with this structural assignment.

L. [^{3}H]Thymidine Incorporation. MCF-7 cells were plated onto 24-well Corning tissue culture dishes. Triplicate samples of asynchronously growing mammary cells were treated for the indicated times with either vehicle control (1 µl DMSO/ml medium) or varying concentrations of I3C and/or tamoxifen. The cells were pulsed for three hours with 3 µCi [^{3}H]thymidine (84 Ci/mmol), washed three times with ice cold 10% trichloroacetic acid, and lysed with 300 µl 0.3 N NaOH. Lysates (150 µl) were transferred into vials containing liquid scintillation cocktail and radioactivity was quantitated by scintillation counting. Triplicates were averaged and expressed as counts per minute per well.

M. Crystal Violet Staining of Low Confluency Cultures. MCF-7 cells were plated onto 100 mm Corning tissue culture dishes (10,000 cells per plate). The cells were treated with the indicated concentrations of I3C and tamoxifen for 8 days. At the end of the treatment, the cells were washed with PBS and incubated in a solution of 0.5% crystal violet and 10% formalin for 10 minutes, then rinsed with water. The integrated density of the colonies on each plate was determined using NIH Image software. The morphology of the cells was examined on a Nikon Axiophot microscope and representative photographs were taken at 200X magnification.

N. Soft Agar Colony Formation Two layers of Difco agar with different concentrations were set in individual wells of a 24 well plate. The lower layer contained 0.5 ml 0.6% soft agar in media with the indicated combinations of I3C and tamoxifen. The upper layer was composed of 0.5 ml 0.3% soft agar in media with MCF-7 cells (500 cells/well) and the corresponding combinations of I3C and tamoxifen in triplicate. After 4.5 weeks, all of the colonies larger than 50 µm in diameter were counted.

O. Flow Cytometric Analyses of DNA Content. MCF-7 cells (4 x 10^4) were plated onto Corning 6-well tissue culture dishes. Triplicate samples were treated with the indicated concentrations of I3C and tamoxifen. The medium was changed every 24 hours. Cells were incubated for 96 hours and hypotonically lysed in 1 ml of DNA staining solution (0.5 mg/ml propidium iodide, 0.1% sodium citrate, 0.05% Triton X-100). Nuclear emitted fluorescence with wavelength greater than 585 nM was measured with a Coulter Elite instrument with laser output adjusted to deliver 15 mW at 488 nM. Nuclei (10,000) were analyzed from each sample at a rate of 300-500 nuclei/second. The percentages of cells within the G1, S, and G2/M

phases of the cell cycle were determined by analysis with the Multicycle computer program provided by Phoenix Flow Systems in the Cancer Research Laboratory Microchemical Facility of the University of California, Berkeley.

P. Western Blot Analysis. After the indicated treatments, cells were harvested in RIPA buffer (150 mM NaCl, 0.5% deoxycholate, 0.1% NP-40, 0.1% SDS, 50 mM Tris) containing protease and phosphatase inhibitors (50 μg/ml PMSF, 10 μg/ml aprotinin, 5 μg/ml leupeptin, 0.1 μg/ml NaF, 10 μg/ml β-glycerophosphate). Equal amounts of total cellular protein were mixed with loading buffer (25% glycerol, 0.075% SDS, 1.25 ml 14.4 M 2-mercaptoethanol, 10% bromophenol blue, 3.13% 0.5 M Tris-HCl; 0.4% SDS; pH 6.8) and fractionated on 10% (7.5% for Rb) polyacrylamide/0.1% SDS resolving gels by electrophoresis. Rainbow marker (Amersham Life Sciences, Arlington Heights, IL) was used as the molecular weight standard. Proteins were electrically transferred to nitrocellulose membranes (Micron Separations, Inc., Westboro, MA) and blocked overnight at 4°C with western wash buffer/5% NFDM (10 mM Tris HCl pH 8.0, 150 mM NaCl, 0.05% Tween 20/5% nonfat dry milk). Blots were subsequently incubated for 1 hour at room temperature for rabbit anti-CDK2, CDK4, CDK6, p21, cyclin D1, and cyclin E antibodies (Santa Cruz Biotechnology, Inc., Santa Cruz, CA Cat. #sc-163, sc-260, sc-177, sc-543 respectively) and overnight at 4°C for mouse anti-Rb antibodies (Pharmingen, San Diego, CA, Cat. # 14001A). Working concentration for all antibodies was 1 μg/ml western wash buffer. Immunoreactive proteins were detected after incubation with horseradish peroxidase-conjugated secondary antibody diluted to 3×10^{-4} in western wash buffer/1% NFDM (goat anti-rabbit IgG, BioRad, Hercules, CA, rabbit anti-mouse IgG, Zymed, SF, CA). Blots were treated with ECL reagents (NEN Life Science Products) and all proteins were detected by autoradiography. Equal protein loading was confirmed by Ponceau S staining of blotted membranes.

Q. Immunopreciptation and CDK Kinase Assay. MCF-7 cells were cultured in growth medium with combinations of tamoxifen and I3C for the indicated times and then rinsed twice with PBS, harvested, and stored as dry pellets at -70°C. For the immunoprecipitation, cells were lysed for 15 minutes in immunoprecipitation (IP) buffer (50 mM Tris HCl pH 7.4, 200 mM NaCl, 0.1% Triton X-100) containing protease and phosphatase inhibitors (50 μg/ml PMSF, 10 μg/ml aprotinin, 5 μg/ml leupeptin, 0.1 μg/ml NaF, 10μg/ml β-glycerophosphate, and 0.1 mM sodium orthovanadate). Samples were diluted to 500 μg protein in 1 ml IP buffer. Samples were pre-cleared for 30 minutes at 4°C with 20 μl of a 1:1 slurry of protein-A sepharose beads (Pharmacia Biotech, Sweden) in IP buffer and 1 μg rabbit IgG. After a brief centrifugation to remove precleared beads, 0.5 μg anti-CDK2 or anti-CDK6 antibody was added to each sample and incubated on a rocking platform at 4°C for 2 hours. Then, 20 μl protein-A sepharose beads were added to each sample and the slurries incubated on the rocking platform at 4°C for 30 minutes. The beads were then washed five times with IP buffer and twice with kinase buffer (50 mM HEPES, 10 mM $MgCl_2$, 5 mM $MnCl_2$, 0.1 μg/ml NaF, 10 μg/ml β-glycerophosphate, and 0.1 mM sodium orthovanadate). Half of the immunoprecipitated sample was checked by western blot analysis to confirm the immunoprecipitation.

For the kinase assay, the other half of the immunoprecipitated sample was resuspended in 25 µl kinase buffer containing 20 mM ATP, 5 mM DTT, 0.21 µg Rb carboxy-terminal domain protein substrate (Santa Cruz Biotechnology, Inc. Cat. # sc-4112), and 10 µCi [γ^{33}P] ATP (3000 Ci/mmol). Reactions were incubated for 15 minutes at 30°C, and stopped by adding an equal volume of 2X loading buffer (10% glycerol, 5% β-mercaptoethanol, 3% SDS, 6.25 mM Tris HCl pH 6.8, and bromophenol blue). Reaction products were boiled for 10 minutes and then electrophoretically fractionated in SDS-10% polyacrylamide gels. Gels were stained with Coomassie blue to monitor loading and de-stained overnight with 3% glycerol in 10% Acetic acid. Subsequently, gels were dried and quantitated on a PhosphorImager (Molecular Dynamics, Sunnyvale, CA) and visualized by autoradiography.

R. Quantitation of Autoradiography. Autoradiographic exposures were scanned with a UMAX UC630 scanner and band intensities were quantified using the NIH Image program. Autoradiographs from a minimum of three independent experiments were scanned per time point.

Conclusions:

We have made several significant observations during this phase of the grant.

a. Our results show that DIM can exhibit both agonist and antagonist activities against proliferation of MCF-7 cells and against transcriptional activation of endogenous and exogenous estrogen-responsive genes. Under conditions were cells are exposed to both DIM and estradiol, the primary effect of DIM is antagonistic of estradiol function and this effect appears to be independent of the Ah receptor (20). Thus, further investigations of its mode of action of DIM in the control of estradiol-induced cell proliferation appear warranted.

b. We report the effects of a second major component of RXM, the linear trimer, 2-(indol-3-ylmethyl)-3,3´-diindolylmethane (LTr-1), in tumor cells. We show that whereas this novel compound is an antagonist of estrogen receptor function with little agonist activity, it also inhibits proliferation of both estrogen dependent and independent cultured breast tumor cells (21). Further studies of the antiproliferative effects of LTr-1 are in progress.

c. We demonstrate that I3C and tamoxifen work through different signal tranduction pathways to suppress the growth of human breast cancer cells. Most significantly, a combination of tamoxifen and I3C displayed a more effective growth suppression response, more stringent inhibition of CDK2 specific activity, and endogenous Rb phosphorylation compared to the effects of either compound alone (22). Our results suggest the possibility of developing I3C and tamoxifen as a potential combinatorial therapy to control estrogen responsive breast cancers.

References:

1. Bradfield, C.A. and Bjeldanes, L.F. (1987) Structure-activity relationships of dietary indoles: a proposed mechanism of action as modifiers of xenobiotic metabolism. J. Toxicol. Environ. Health **21**, 311-323.
2. Bjeldanes, L.F., Kim, J.Y., Grose, K.R., Bartholomew, J.C. and Bradfield, C.A. (1991) Aromatic hydrocarbon responsiveness-receptor agonists generated from indole-3-carbinol in vitro and in vivo: comparisons with TCDD. Proc. Natl. Acad. Sci USA **88**, 9543-9547.

3. Wattenberg, L.W. and Loub, W.D. (1978) Inhibition of polycyclic aromatic hydrocarbon-induced neoplasia by naturally occurring indoles. Cancer Res. **38**, 1410-1415.
4. Shertzer, H.G. (1984) Indole-3-carbinol protects against covalent binding of benzo[a]pyrene and N-nitrosodimethylamine metabolites to mouse liver macromolecules. Chemico-Biol. Interactions **48**, 81-90.
5. Bailey, G.S., Hendricks, J.D., Shelton, K.W., Nixon, J.E. and Pawlowski, N.E. (1987) Enhancement of carcinogenesis by the natural anticarcinogen indole-3-carbinol. J. Natl. Cancer Inst. **78**, 931-936.
6. Shertzer, H.G. (1983) Protection by indole-3-carbinol against covalent binding of benzo[a]pyrene metabolites to mouse liver DNA and protein. Food Chem. Toxicol. **21**, 31-36.
7. Dashwood, R.H., Arbogast, D.N., Fong, A.T., Hendricks, J.D. and Bailey, G.S. (1988) Mechanisms of anticarcinogenesis by indole-3-carbinol: detailed in vivo DNA binding dose-response studies after dietary administration with aflatoxin B1. Carcinogenesis **9**, 427-430.
8. Sharma, S., Stutzman, J., Kelloff, G. and Steele, V. (1994) Screening of potential chemopreventive agents using biochemical markers of carcinogenesis. Cancer Res. **54**, 5848-5855.
9. Bradlow, H.L., Michnovicz, J.J., Telang, N.T., and Osborne, M.P. (1991) Effects of dietary indole-3-carbinol on estradiol metabolism and spontaneous mammary tumors in mice. Carcinogenesis **12**, 1571-1574.
10. Michnovicz, J.J. and Bradlow, H.L. (1990) Induction of estradiol metabolism by dietary indole-3-carbinol in humans. J. Natl. Cancer Inst. **82**, 947-951.
11. Jellinck, P.H., Forket, P.G., Riddick, D.S., Okey, A.B., Michnovicz, J.J. and Bradlow, H.L. (1993) Ah receptor binding properties of indole carbinols and induction of hepatic estradiol hydroxylation. Biochem. Pharmacol. **43**, 1129-1136.
12. Lubet, R. National Cancer Institute, personal communication.
13. Wattenberg, L.W. (1990) Inhibition of carcinogenesis by naturally occurring and synthetic compounds. In: Antimutagenesis and Anti-carcinogenesis Mechanisms II, Kuroda, Y., Shankel, D.M., and Waters, M.D., Eds., Plenum Press, New York.
14. Tiwari, R. K., Li Guo, H., Bradlow, Leon, Telang, N.T., and Osborne, M.P. (1994) Selective responsiveness of human breast cancer cells to indole-3-carbinol, a chemopreventive agent. J. Natl. Cancer Inst. **86**, 126-131.
15. Cover, C.M., Hsieh, S.J., Tran, S.H., Hallden, G., Kim, G.S., Bjeldanes, L.F., Firestone, G.L. (1998) Indole-3-carbinol inhibits the expression of cyclin-dependent kinase-6 and induces a G1 cell cycle arrest of human breast cancer cells independent of estrogen receptor signaling. J. Biol. Chem. **273**:3838-47.
16. de Kruif, C.A., Marsman, J.W., Venekamp, J.C., Falke, H.E., Noordhoek, J., Blaauboer, B.J., and Wortelboer, H.M. (1991) Structure elucidation of acid reaction products of indole-3-carbinol: detection in vivo and enzyme induction in vitro. Chem.-Biol. Interact. **80**, 303-315.
17. Bardon, S., Vignon, F., Derocq, D., and Rochefort, H. (1984) The antiproliferative effect of tamoxifen in breast cancer cells: mediation by the estrogen receptor. Mol. Cell. Endocrinol. **35**:89-96.
18. Sherr, C. J. (1996) Cancer cell cycles. Science, **274**: 1672-1677.

19. Grose, K.R., and Bjeldanes, L.F. (1992) Oligomerization of indole-3-carbinol in aqueous acid. Chem. Res. Toxicol. **5**, 188-193.
20. Riby, J.E., Chang, G., Firestone, G. and Bjeldanes, L. (1998) Estrogen Receptor Agonist and Antagonist Activity of 3,3'-Diindolylmethane in MCF7 Human Breast Cancer Cells. Submitted for publication.
21. Chang, Y.-C., Riby, J., Chang, G., Peng, B., Firestone, G. and Bjeldanes, L. (1998) 2-(Indol-3-ylmethyl)-3,3´-diindolylmethane is a Major Cytostatic and Antiestrogenic Product of Dietary Indole-3-carbinol. Submitted for publication.
22. Cover, C., Hsieh, S., Cram, E., Hong, C., Riby, J., Bjeldanes, L., and Firestone, G. (1998) Indole-3-Carbinol and tamoxifen cooperate to arrest the cell cycle of MCF-7 human breast cancer cells. Submitted for publication.

Figure 1

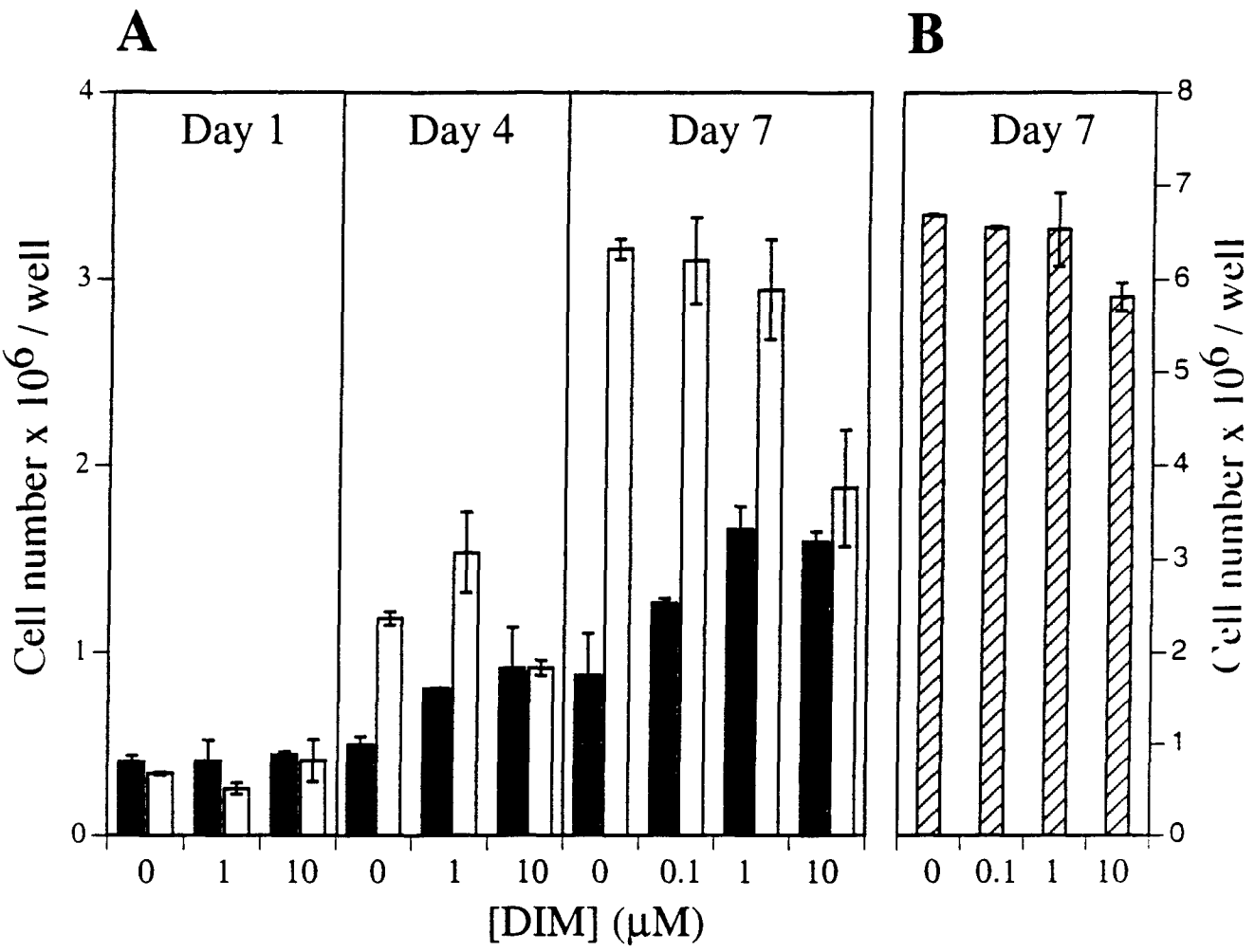
A
B
Day 1
Day 4
Day 7
Day 7
Cell number x 10^6 / well
Cell number x 10^6 / well
0
1
2
3
4
5
6
7
8
0 1 10 0 1 10 0 0.1 1 10
0 0.1 1 10
[DIM] (μM)

Figure 2

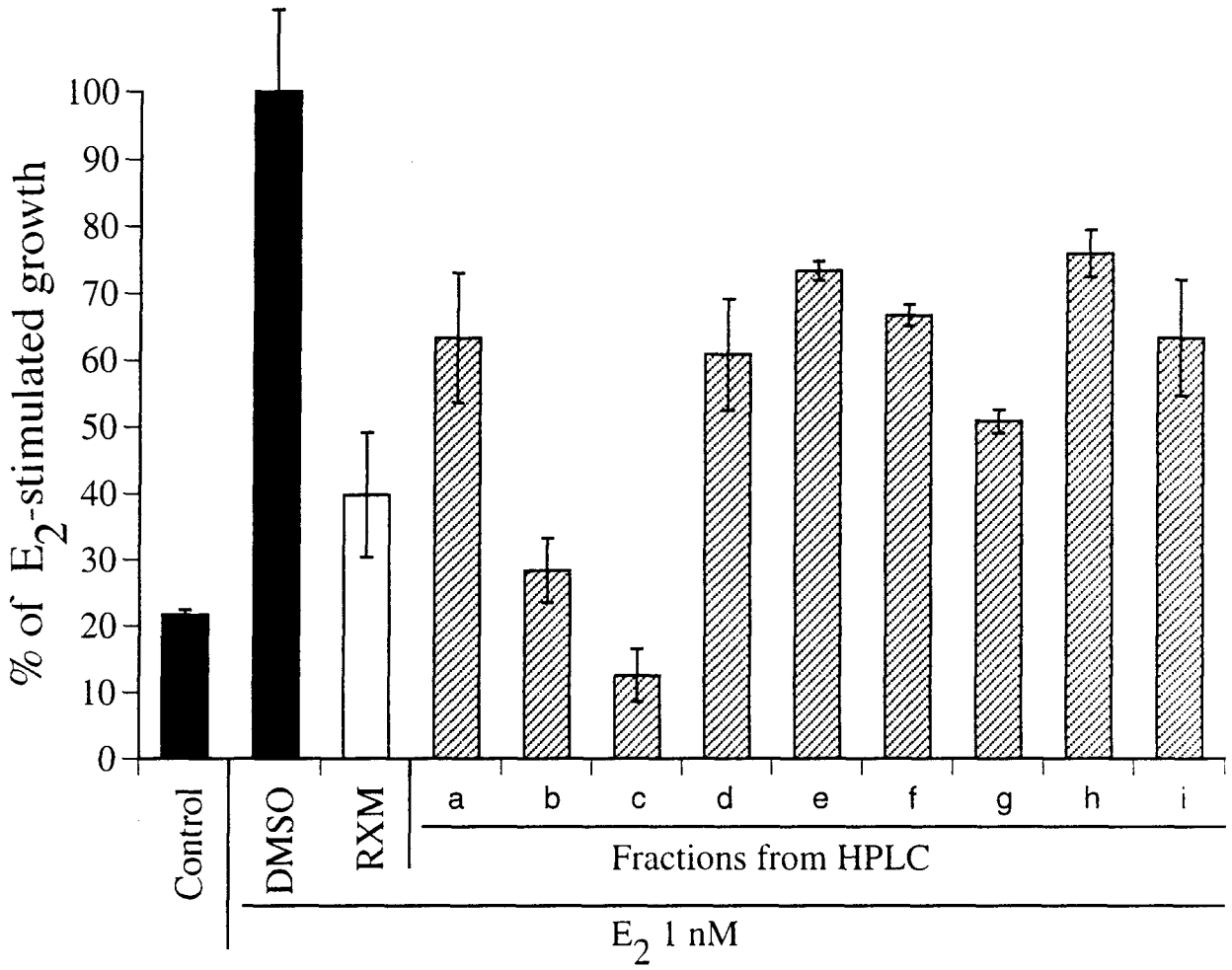
% of E_2-stimulated growth
100
90
80
70
60
50
40
30
20
10
0
Control
DMSO
RXM
a
b
c
d
e
f
g
h
i
Fractions from HPLC
E_2 1 nM

Figure 3

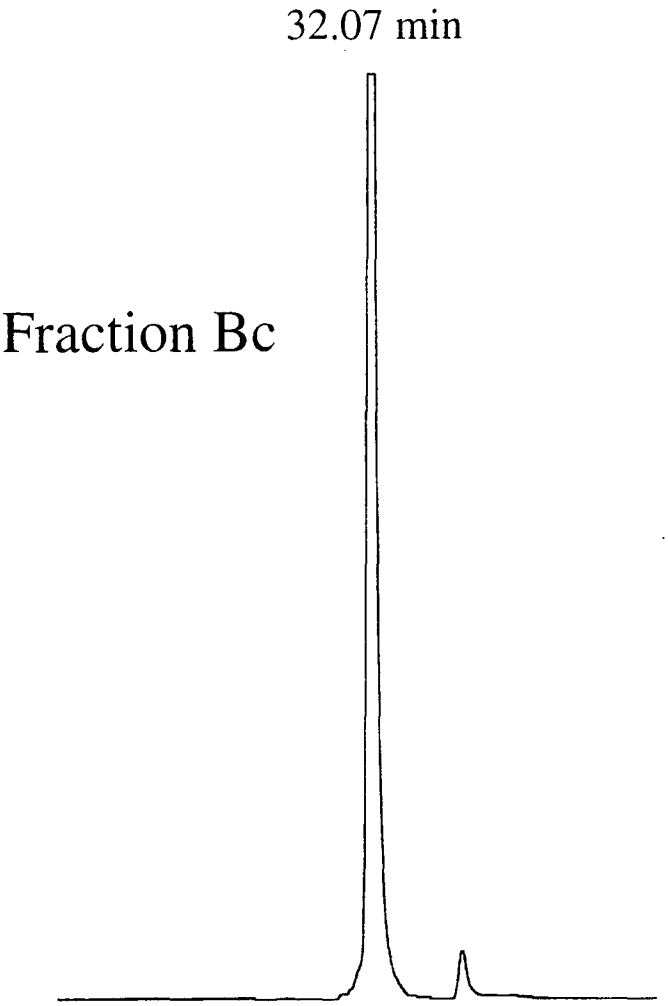

Figure 4

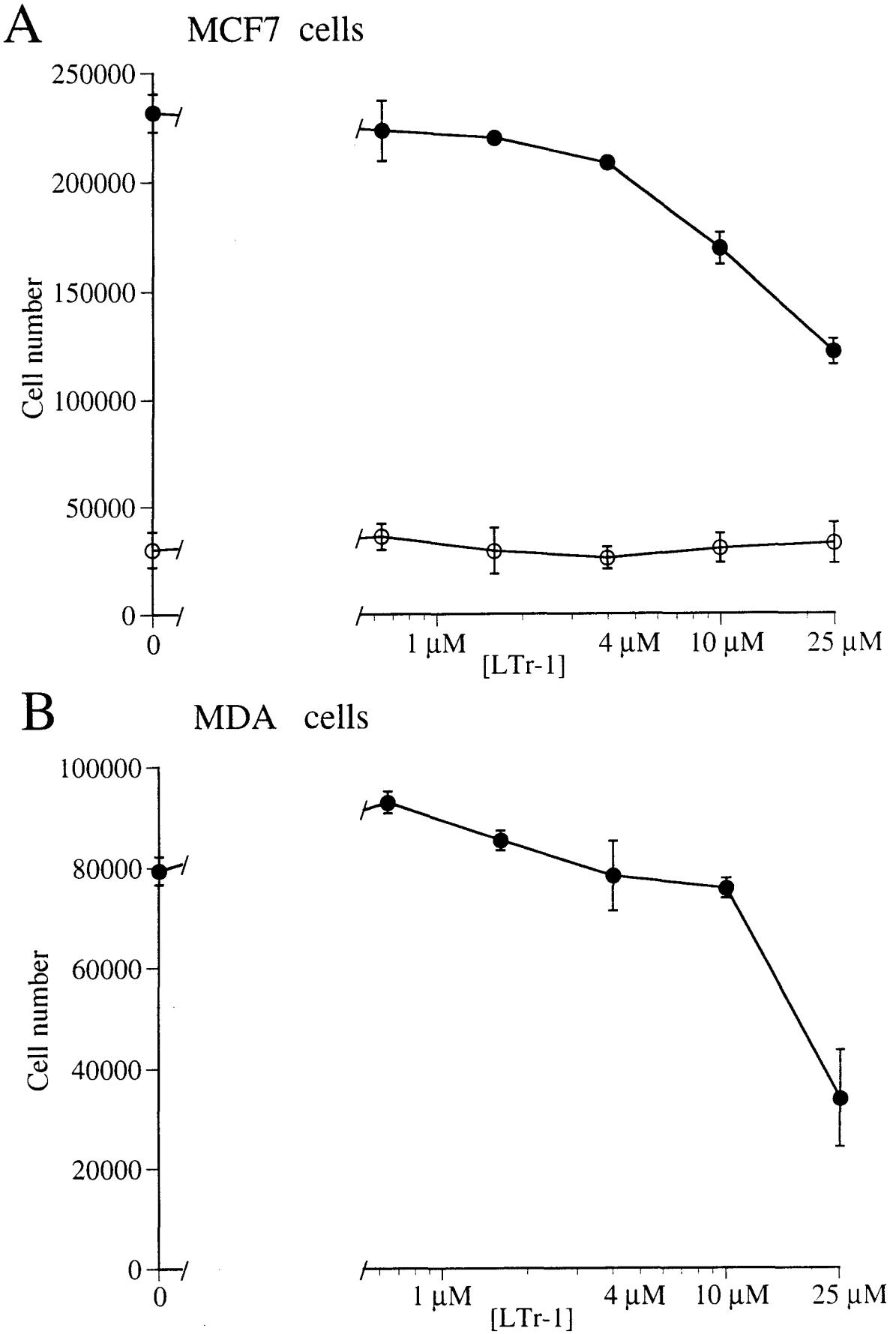
A
MCF7 cells
250000
200000
150000
100000
50000
0
Cell number
0
1 µM
4 µM
10 µM
25 µM
[LTr-1]
B
MDA cells
100000
80000
60000
40000
20000
0
Cell number
0
1 µM
4 µM
10 µM
25 µM
[LTr-1]

Figure 5

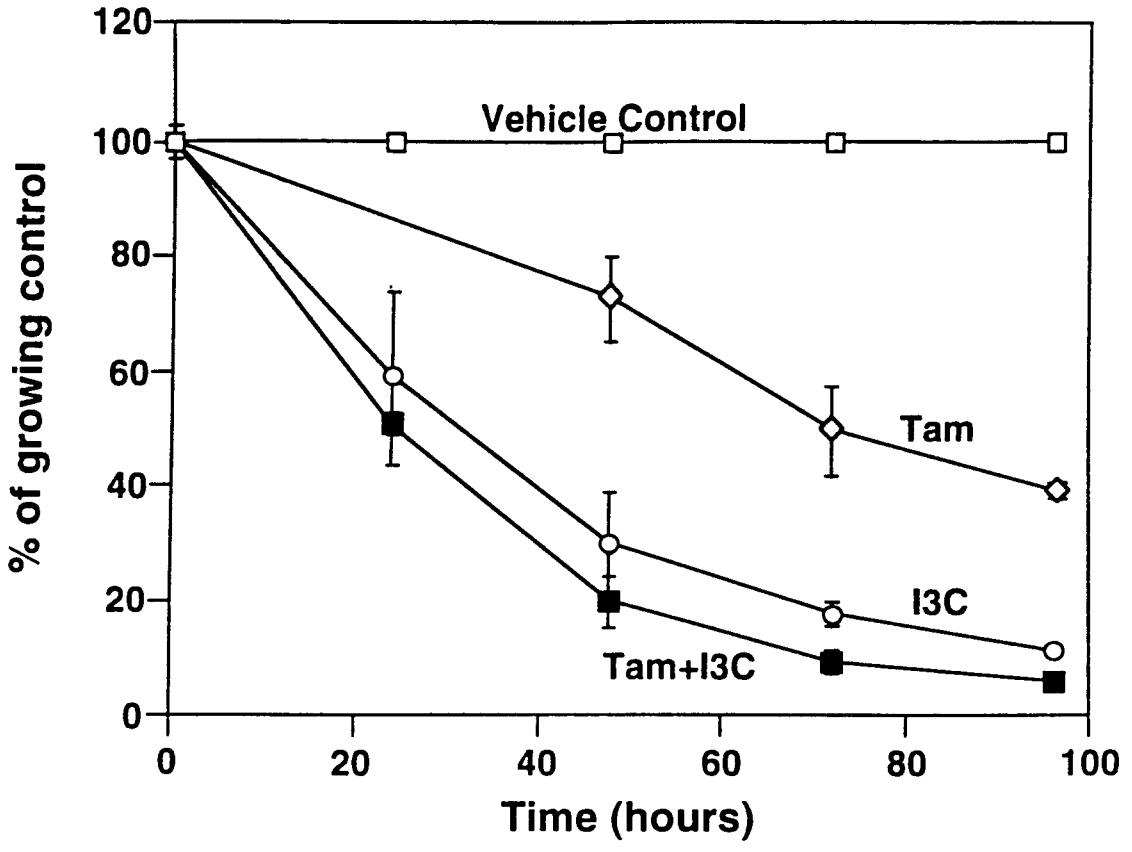
120
100
80
60
40
20
0
% of growing control
Vehicle Control
Tam
I3C
Tam+I3C
0
20
40
60
80
100
Time (hours)

Figure 6

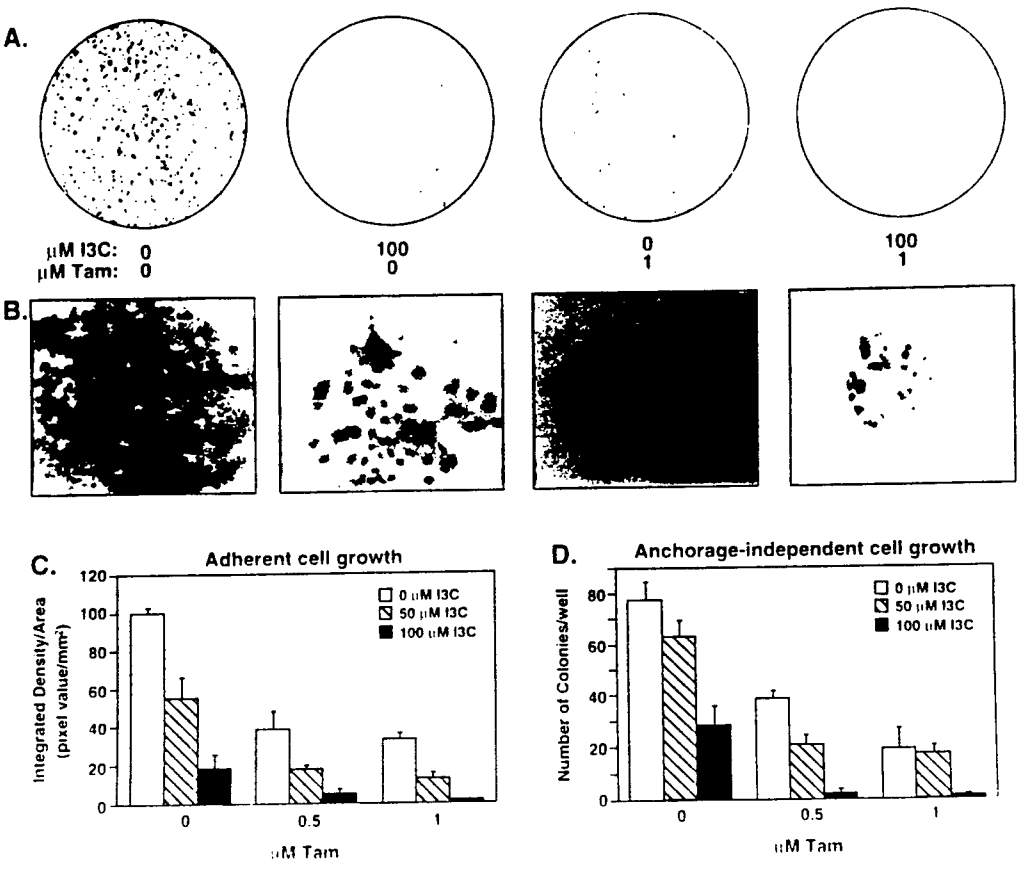
A.
μM I3C: 0
μM Tam: 0
100
0
0
1
100
1
B.
C.
Adherent cell growth
Integrated Density/Area (pixel value/mm²)
0 μM I3C
50 μM I3C
100 μM I3C
0
0.5
1
μM Tam
D.
Anchorage-independent cell growth
Number of Colonies/well
0 μM I3C
50 μM I3C
100 μM I3C
0
0.5
1
μM Tam

Figure 7

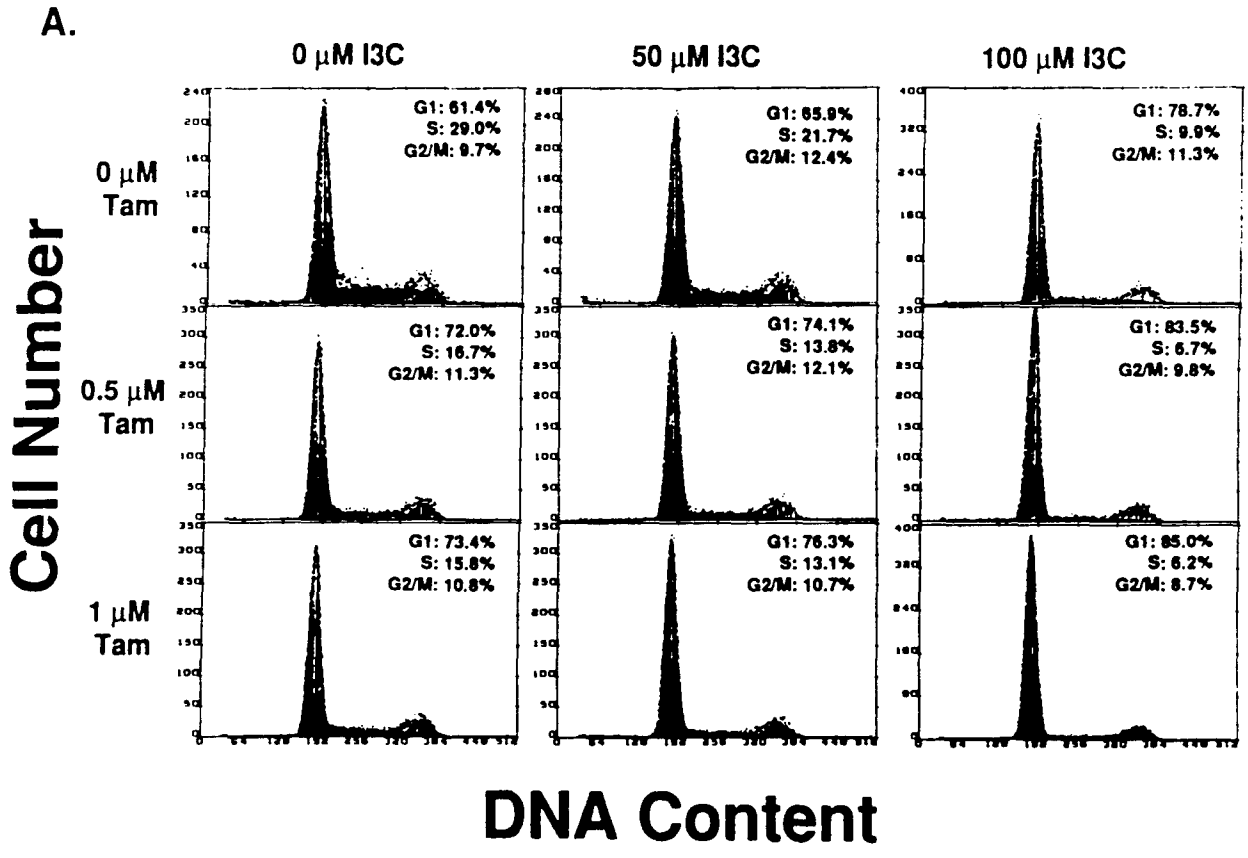
A.
0 μM I3C
50 μM I3C
100 μM I3C
0 μM Tam
0.5 μM Tam
1 μM Tam
G1: 61.4%
S: 29.0%
G2/M: 9.7%
G1: 65.9%
S: 21.7%
G2/M: 12.4%
G1: 78.7%
S: 9.9%
G2/M: 11.3%
G1: 72.0%
S: 16.7%
G2/M: 11.3%
G1: 74.1%
S: 13.8%
G2/M: 12.1%
G1: 83.5%
S: 6.7%
G2/M: 9.8%
G1: 73.4%
S: 15.8%
G2/M: 10.8%
G1: 76.3%
S: 13.1%
G2/M: 10.7%
G1: 85.0%
S: 6.2%
G2/M: 8.7%
Cell Number
DNA Content

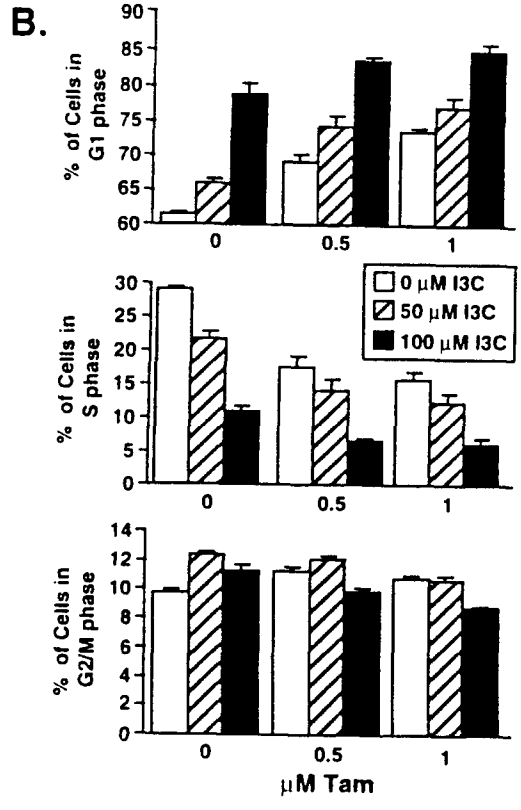
B.
% of Cells in G1 phase
% of Cells in S phase
% of Cells in G2/M phase
0 μM I3C
50 μM I3C
100 μM I3C
μM Tam

Figure 8

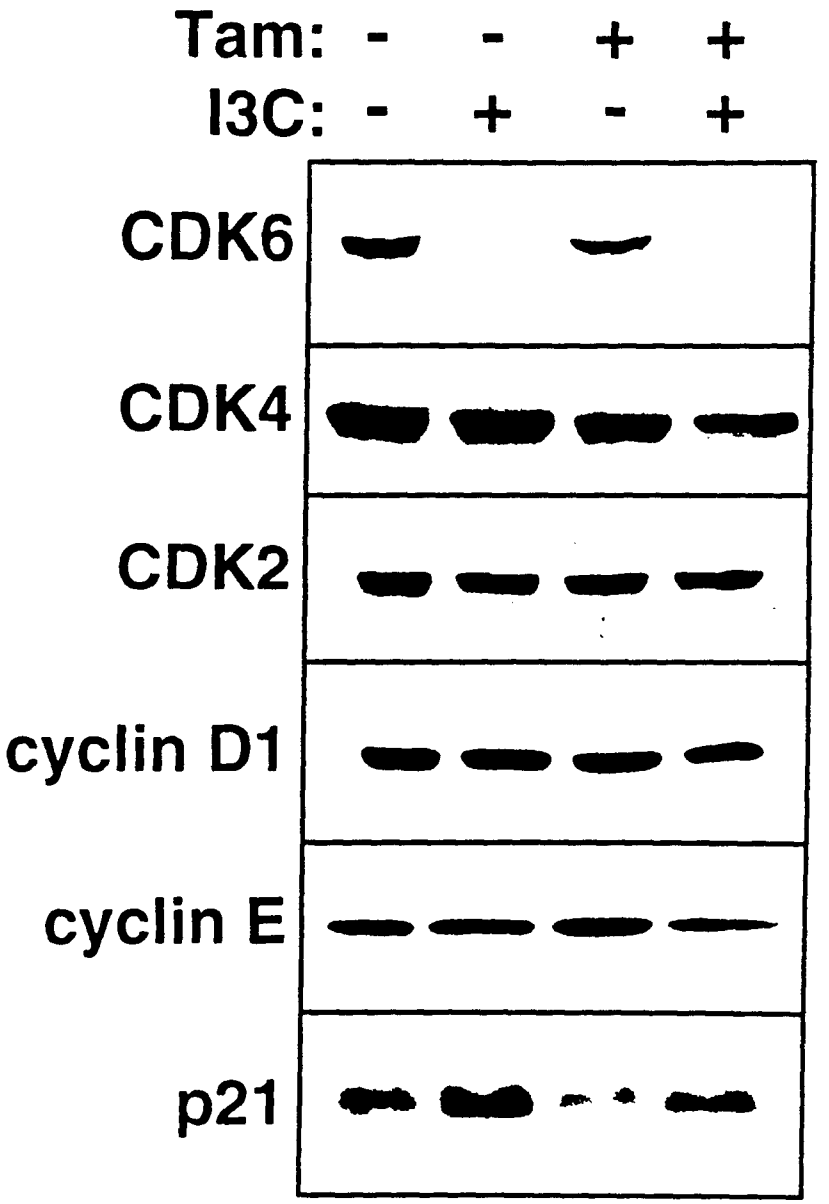

Figure 9

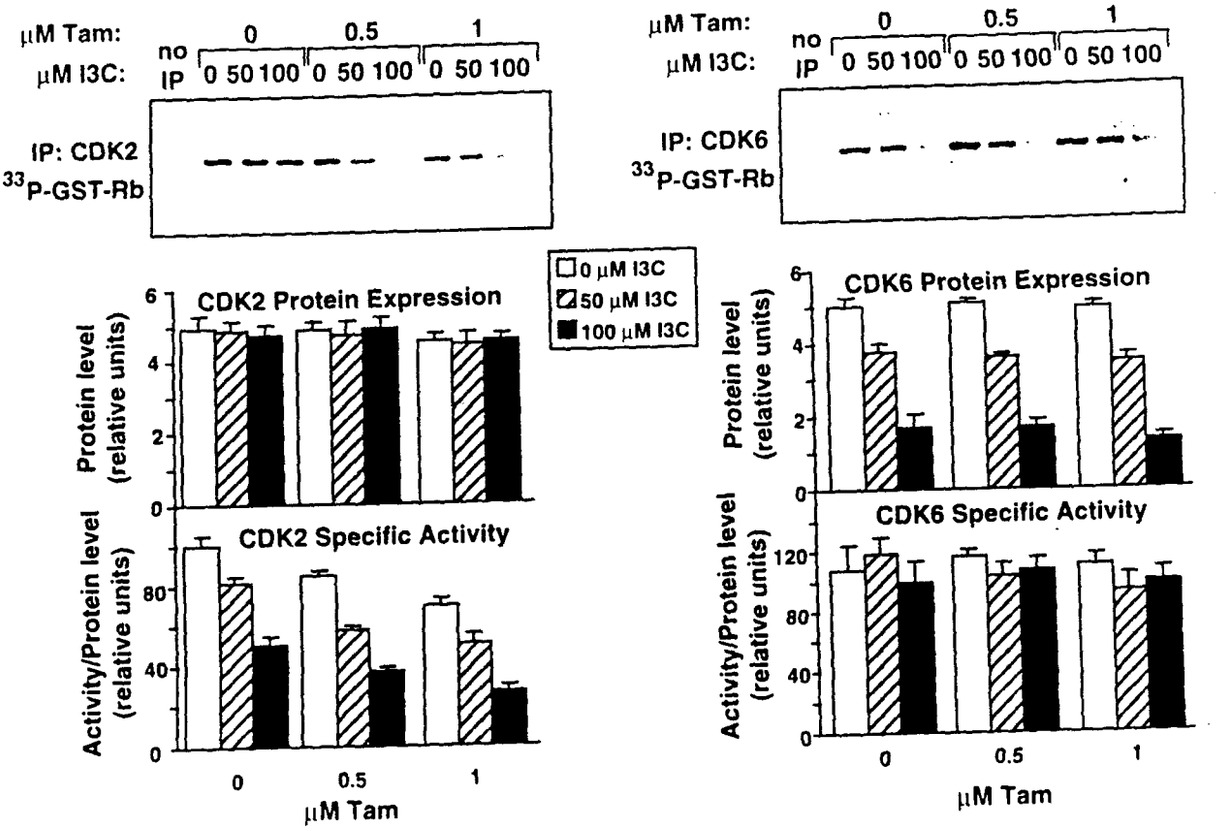
μM Tam:
μM I3C:
no IP
0 50 100 0 50 100 0 50 100
IP: CDK2
33P-GST-Rb
IP: CDK6
0 μM I3C
50 μM I3C
100 μM I3C
CDK2 Protein Expression
CDK6 Protein Expression
Protein level (relative units)
CDK2 Specific Activity
CDK6 Specific Activity
Activity/Protein level (relative units)
μM Tam

Figure 10

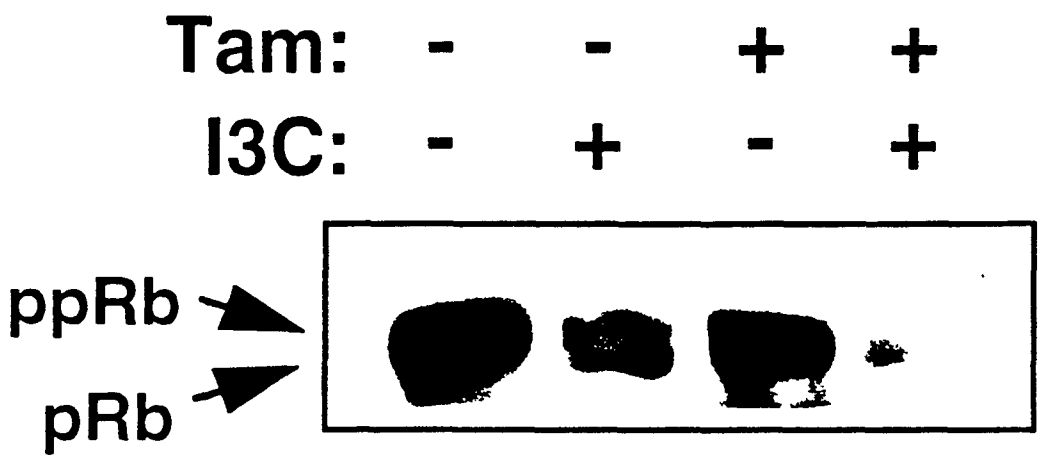

Figure 11

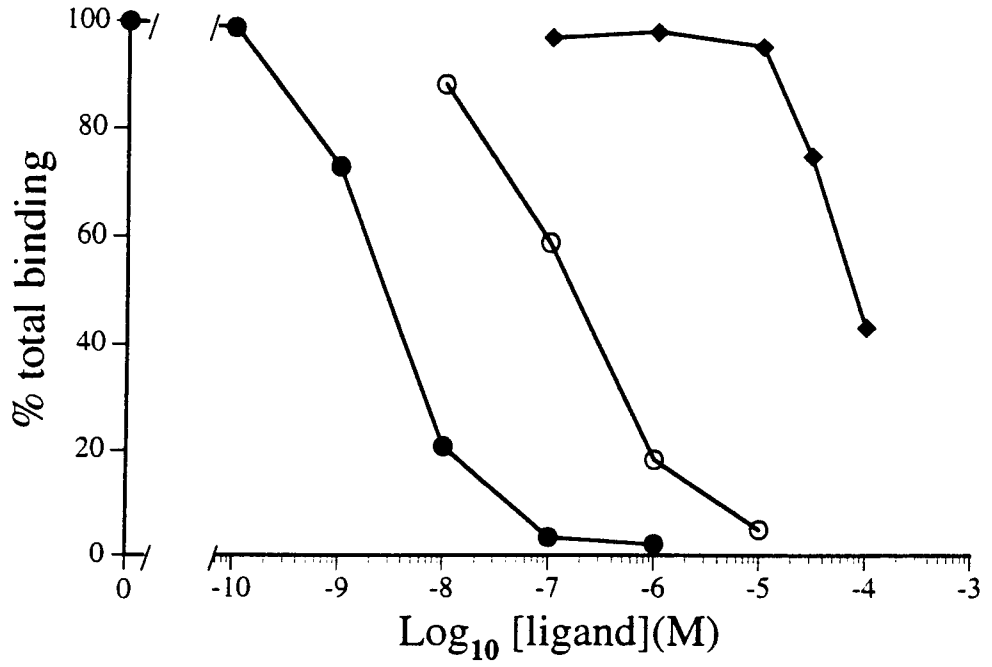

Figure 12

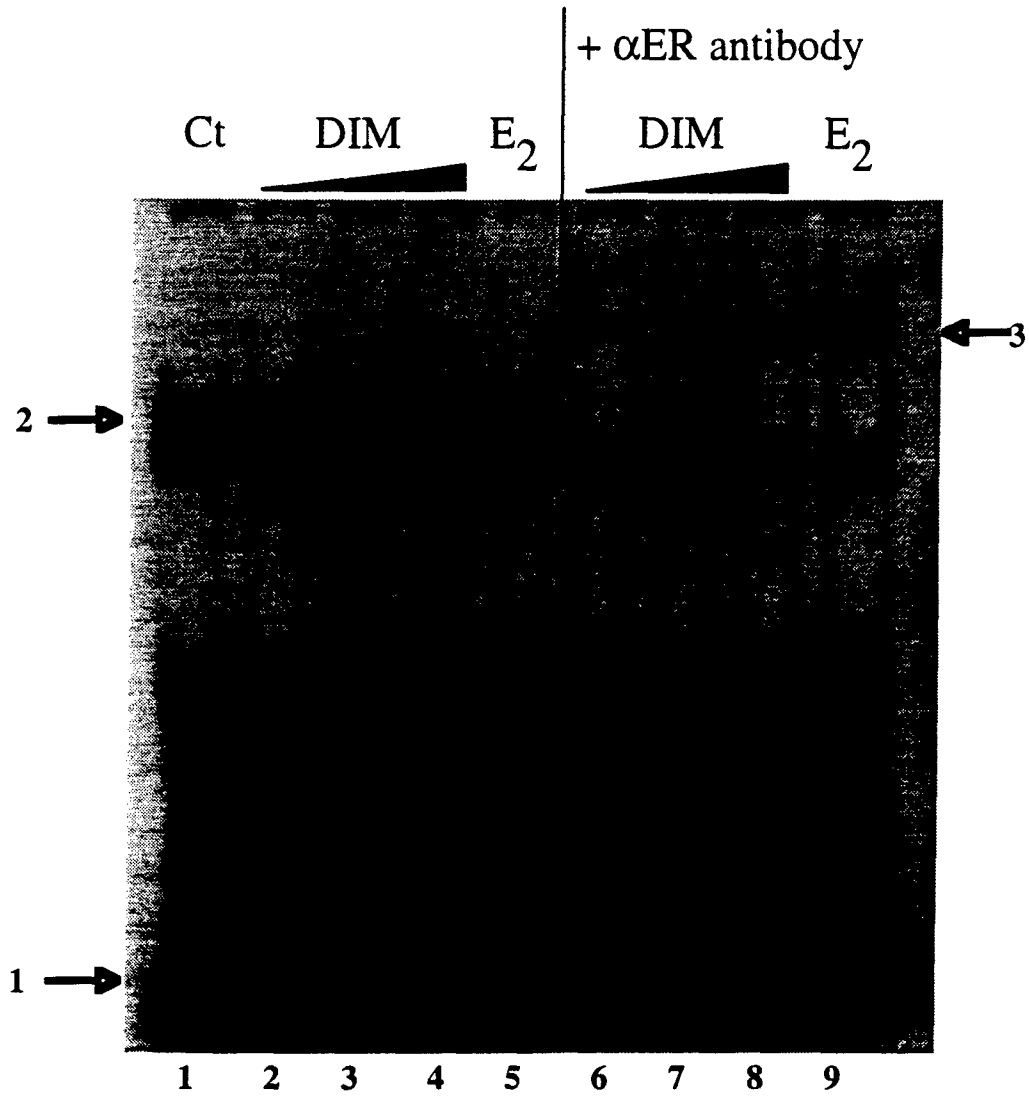

Figure 13

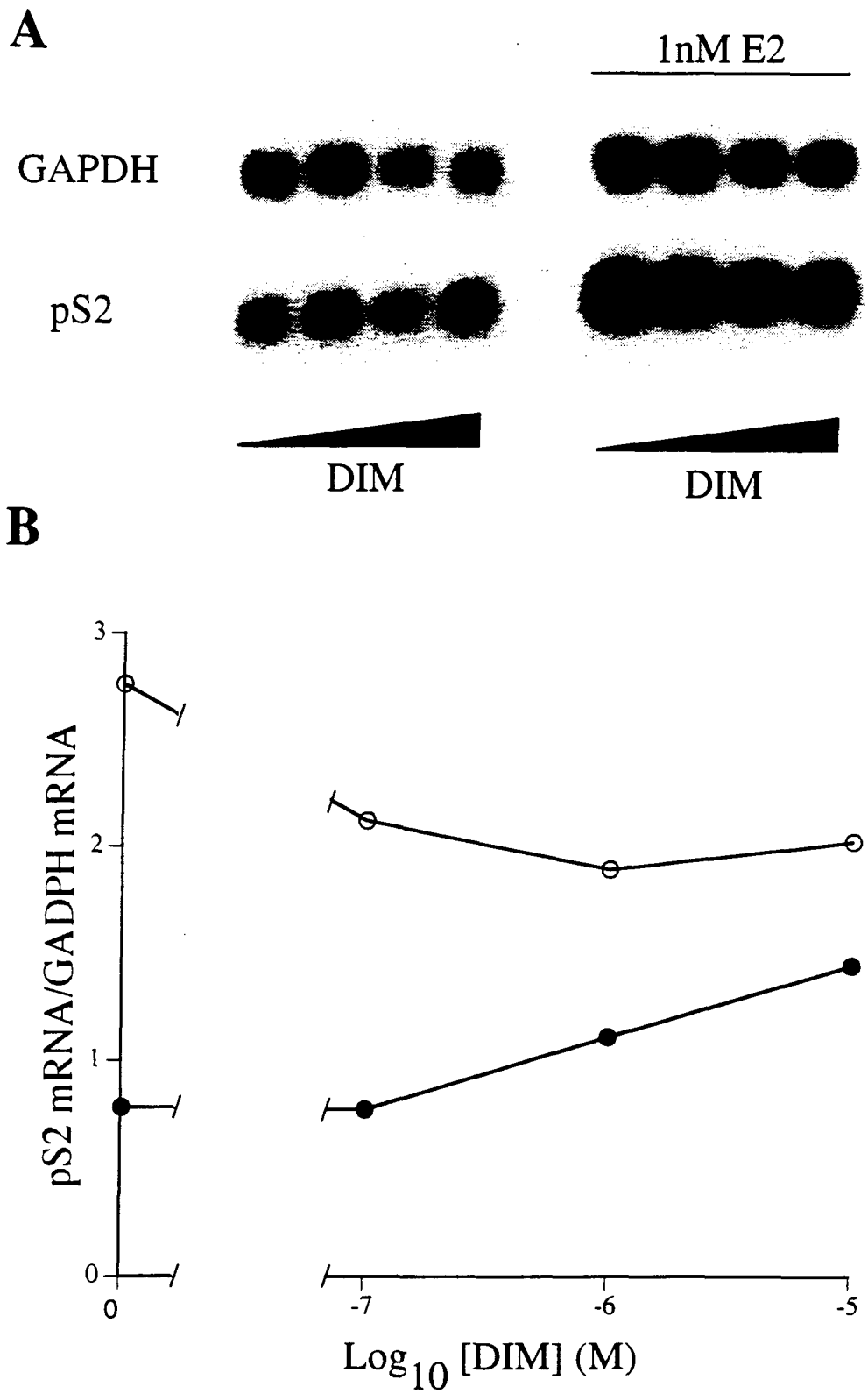
A
1nM E2
GAPDH
pS2
DIM
DIM
B
pS2 mRNA/GADPH mRNA
3
2
1
0
0
-7
-6
-5
Log10 [DIM] (M)

Figure 14

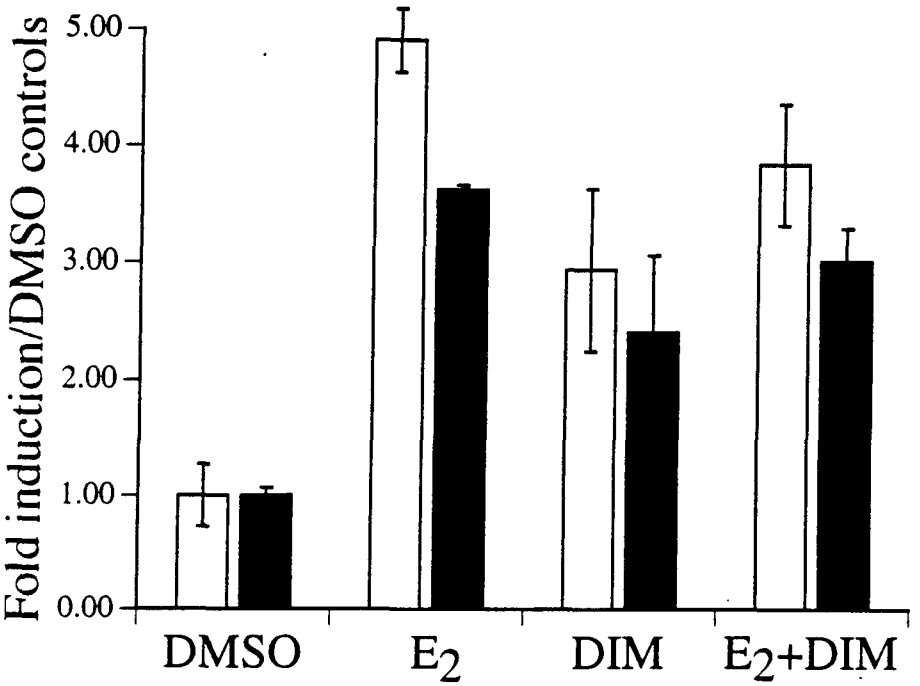
Fold induction/DMSO controls
5.00
4.00
3.00
2.00
1.00
0.00
DMSO
E2
DIM
E2+DIM

Figure 15

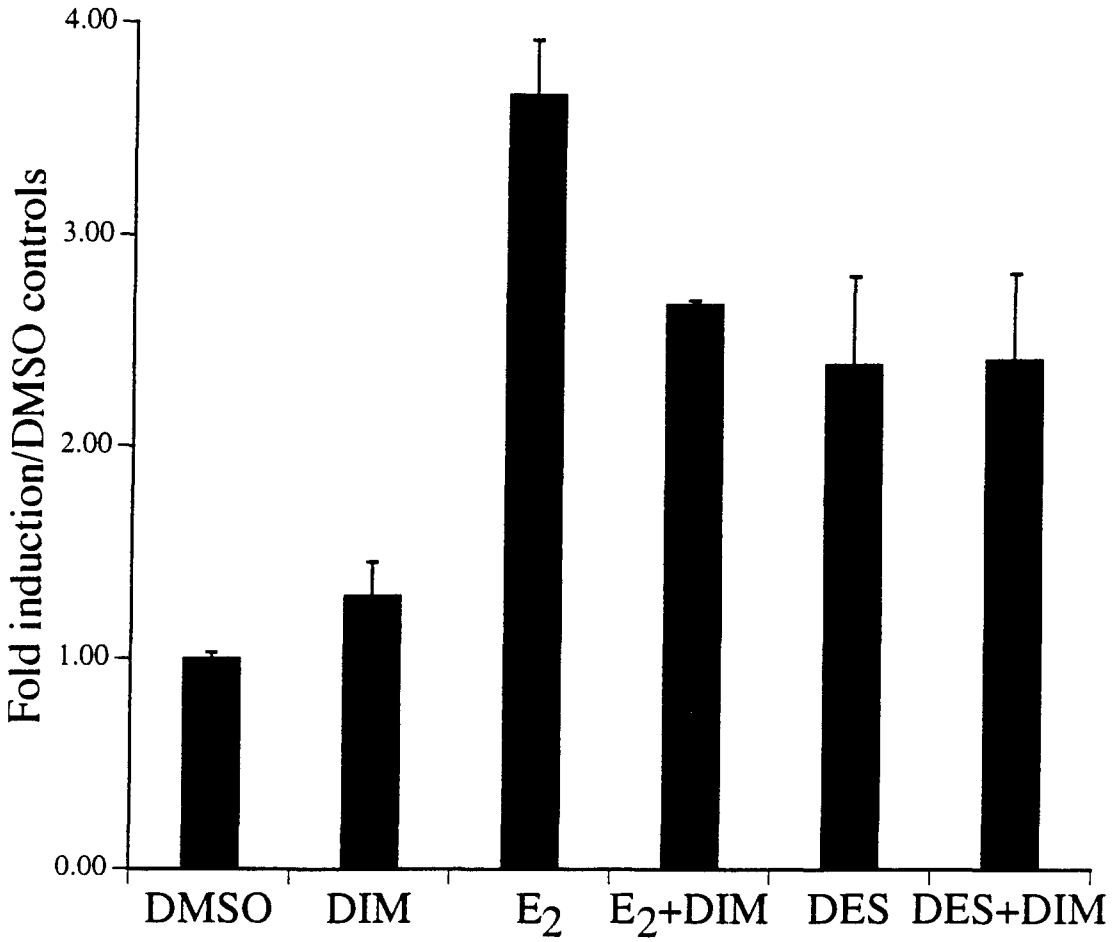
Fold induction/DMSO controls
4.00
3.00
2.00
1.00
0.00
DMSO
DIM
E2
E2+DIM
DES
DES+DIM

Figure 16

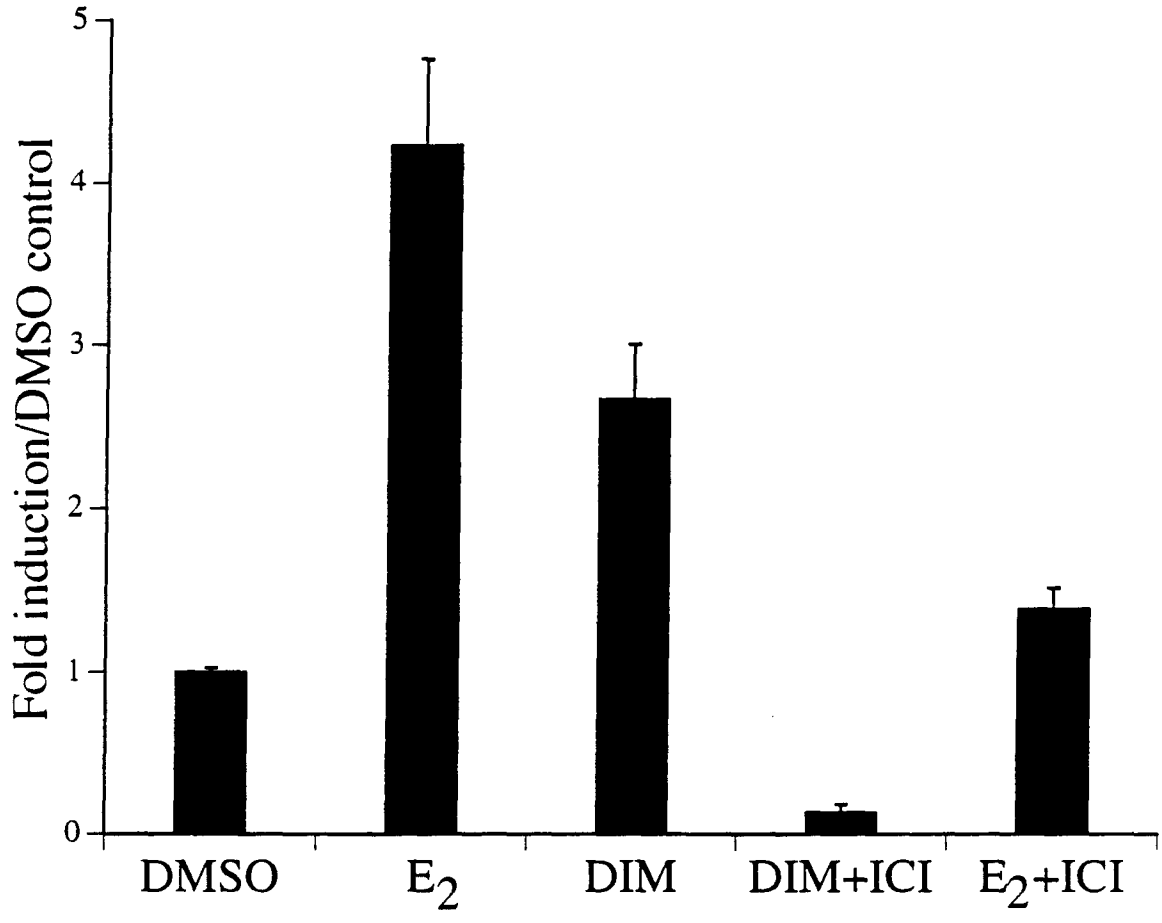
Fold induction/DMSO control
5
4
3
2
1
0
DMSO
E2
DIM
DIM+ICI
E2+ICI

Figure 17

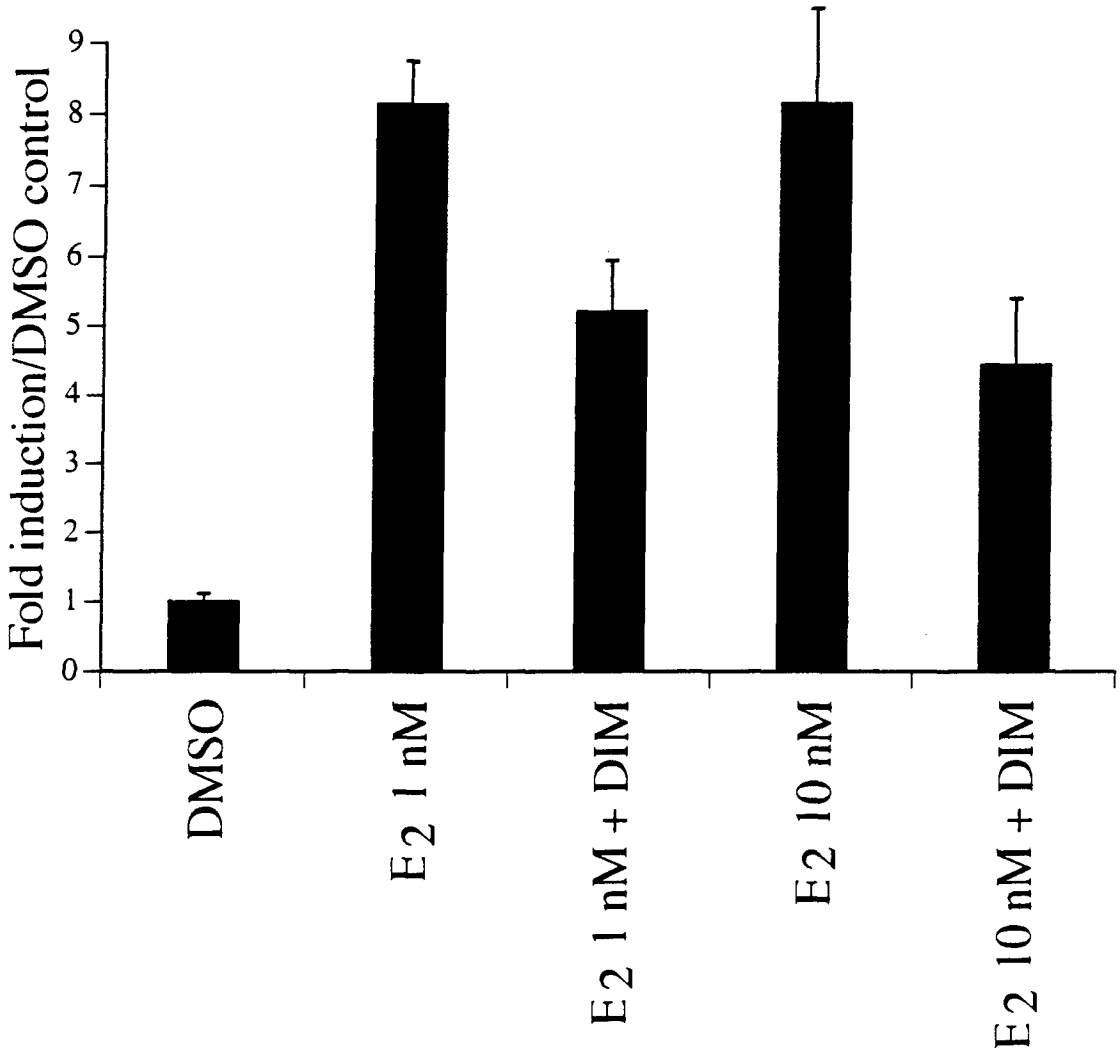
Fold induction/DMSO control
0
1
2
3
4
5
6
7
8
9
DMSO
E2 1 nM
E2 1 nM + DIM
E2 10 nM
E2 10 nM + DIM

Figure 18

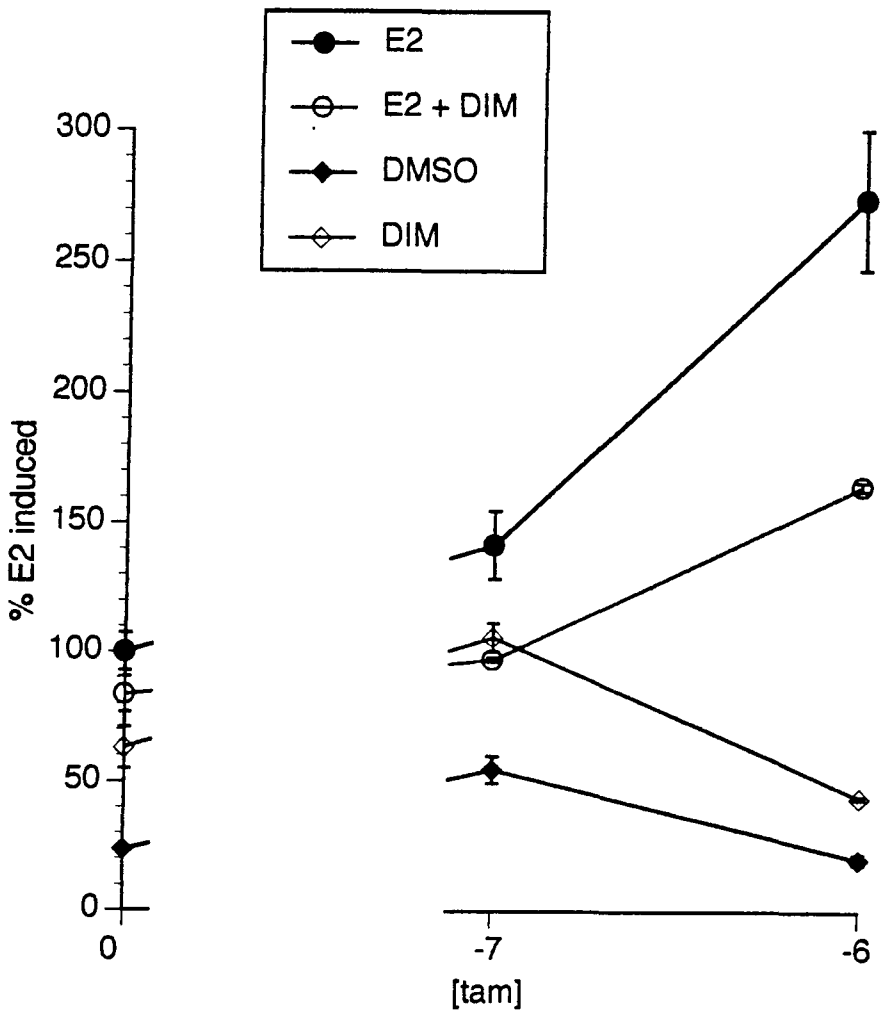

Figure 19

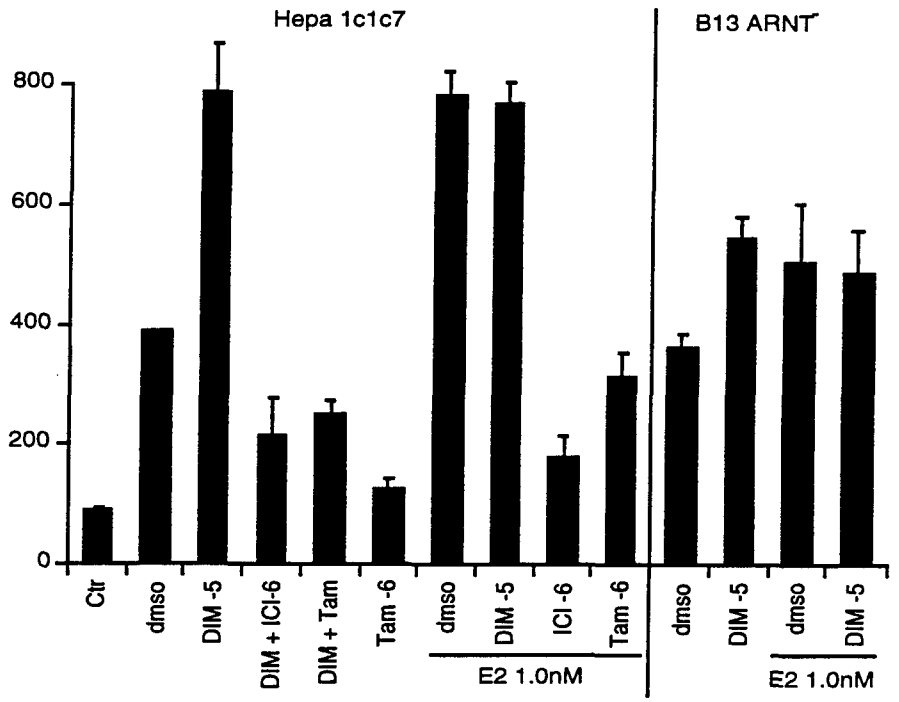
Hepa 1c1c7
B13 ARNT
800
600
400
200
0
Ctr
dmso
DIM -5
DIM + ICI-6
DIM + Tam
Tam -6
dmso
DIM -5
ICI -6
Tam -6
E2 1.0nM
dmso
DIM -5
dmso
DIM -5
E2 1.0nM

Figure 20

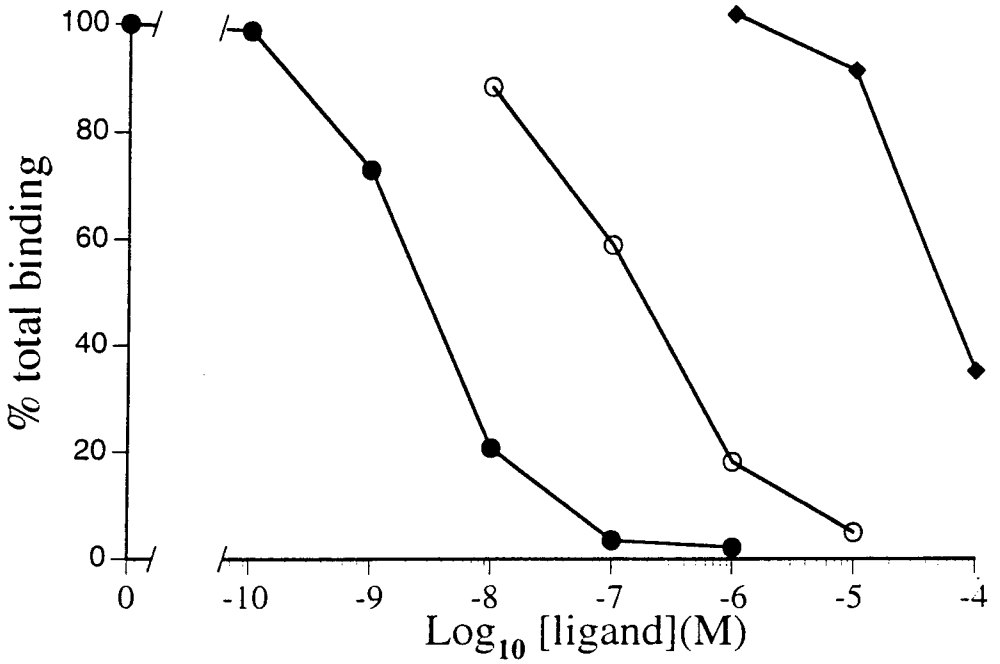

Figure 21

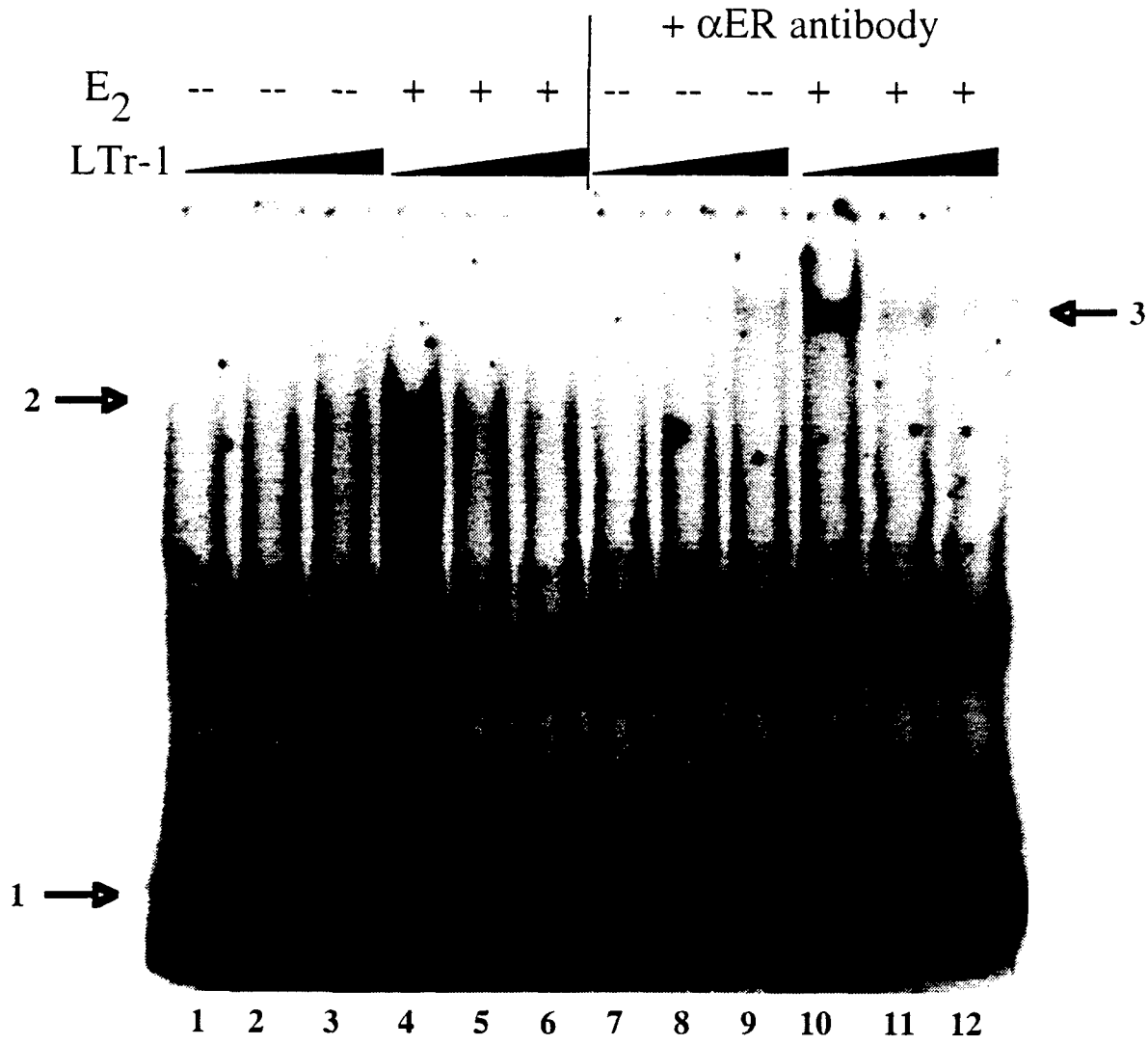

Figure 22

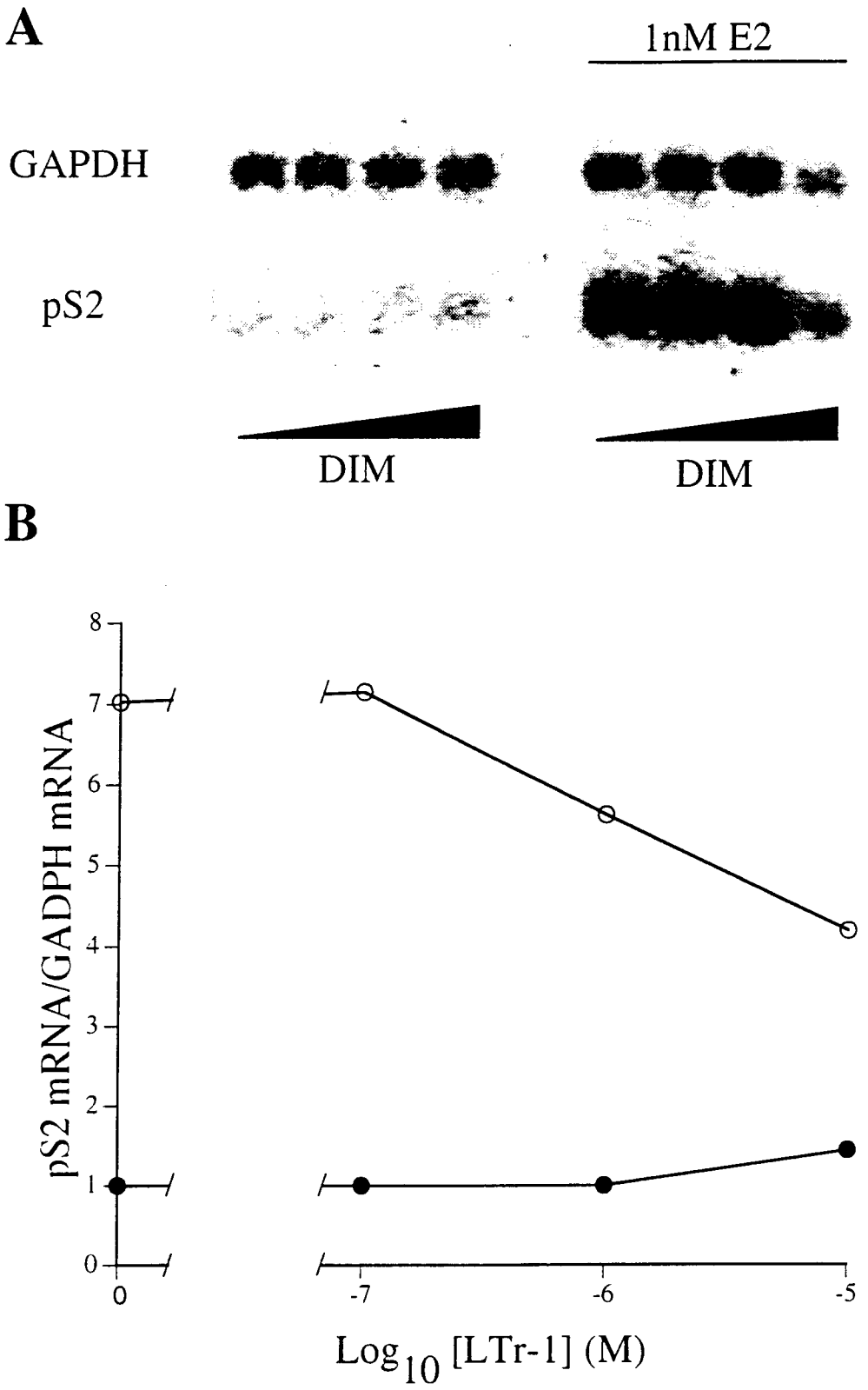
A
1nM E2
GAPDH
pS2
DIM
DIM
B
pS2 mRNA/GADPH mRNA
8
7
6
5
4
3
2
1
0
0
-7
-6
-5
Log10 [LTr-1] (M)

Figure 23

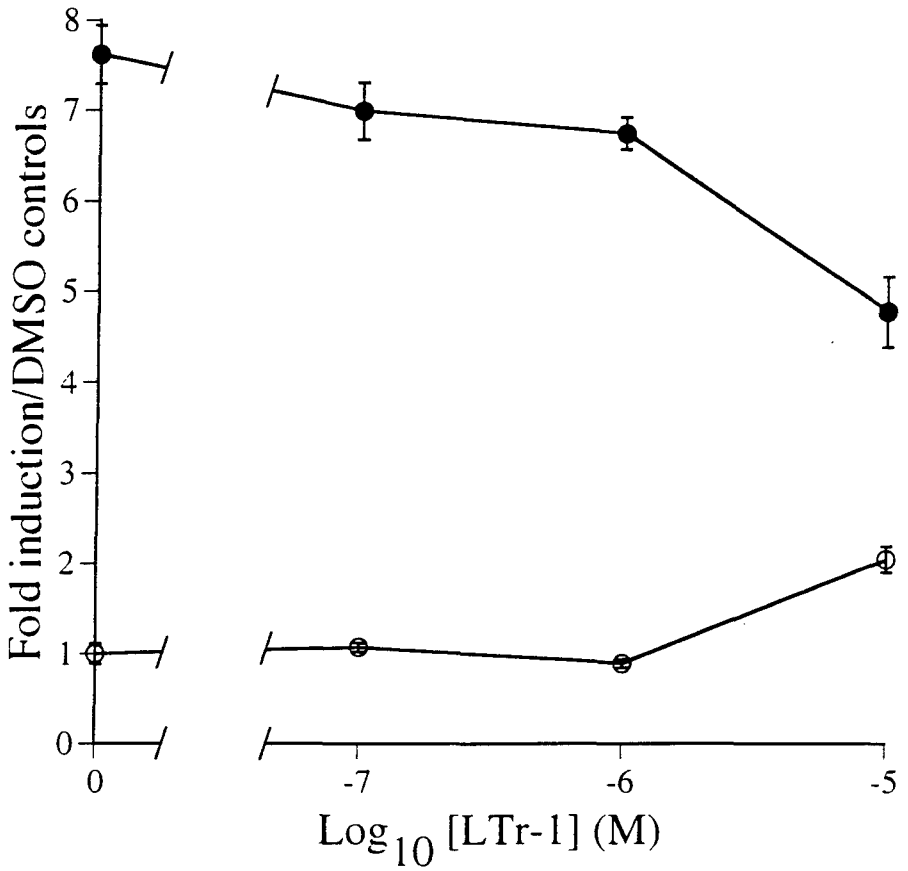

Figure 24

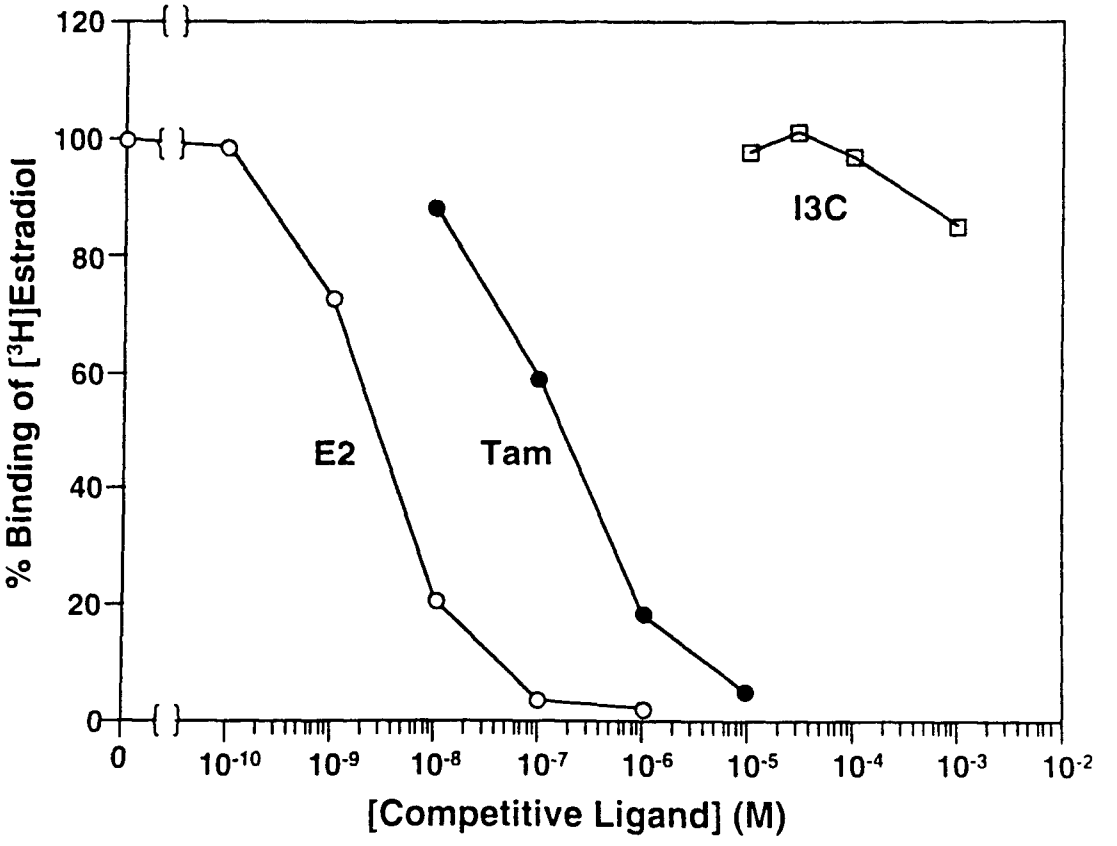
120
100
80
60
40
20
0
% Binding of [3H]Estradiol
E2
Tam
I3C
0
10-10
10-9
10-8
10-7
10-6
10-5
10-4
10-3
10-2
[Competitive Ligand] (M)

DEPARTMENT OF THE ARMY
US ARMY MEDICAL RESEARCH AND MATERIEL COMMAND
504 SCOTT STREET
FORT DETRICK, MARYLAND 21702-5012

REPLY TO
ATTENTION OF:

MCMR-RMI-S (70-1y) 23 Aug 01

MEMORANDUM FOR Administrator, Defense Technical Information Center (DTIC-OCA), 8725 John J. Kingman Road, Fort Belvoir, VA 22060-6218

SUBJECT: Request Change in Distribution Statement

1. The U.S. Army Medical Research and Materiel Command has reexamined the need for the limitation assigned to the technical reports listed at enclosure. Request the limited distribution statement for these reports be changed to "Approved for public release; distribution unlimited." These reports should be released to the National Technical Information Service.

2. Point of contact for this request is Ms. Judy Pawlus at DSN 343-7322 or by e-mail at judy.pawlus@det.amedd.army.mil.

FOR THE COMMANDER:

Encl

PHYLIS M. RINEHART
Deputy Chief of Staff for
Information Management

Reports to be Downgraded to Unlimited Distribution

ADB241560	ADB253628	ADB249654	ADB263448
ADB251657	ADB257757	ADB264967	ADB245021
ADB263525	ADB264736	ADB247697	ADB264544
ADB222448	ADB255427	ADB263453	ADB254454
ADB234468	ADB264757	ADB243646	
ADB249596	ADB232924	ADB263428	
ADB263270	ADB232927	ADB240500	
ADB231841	ADB245382	ADB253090	
ADB239007	ADB258158	ADB265236	
ADB263737	ADB264506	ADB264610	
ADB239263	ADB243027	ADB251613	
ADB251995	ADB233334	ADB237451	
ADB233106	ADB242926	ADB249671	
ADB262619	ADB262637	ADB262475	
ADB233111	ADB251649	ADB264579	
ADB240497	ADB264549	ADB244768	
ADB257618	ADB248354	ADB258553	
ADB240496	ADB258768	ADB244278	
ADB233747	ADB247842	ADB257305	
ADB240160	ADB264611	ADB245442	
ADB258646	ADB244931	ADB256780	
ADB264626	ADB263444	ADB264797	